

The Islamic University of Gaza
Graduate Studies - Faculty of Engineering
Electrical Engineering Department

Bidirectional Radio over Fiber Transmission System Using Reflective Semiconductor Optical Amplifier

"نظام الارسال التناهي لموجات الراديو عبر الألياف الضوئية باستخدام
المكبر الشبه موصل العاكس الضوئي "

A Thesis Presented by:

Mamoun A. A. Salha

Under Supervision of:

Dr. Fady El-Nahal

A Thesis Submitted in Partial Fulfillment of the Requirements for the Degree of
Master in Electrical Engineering

April, 2012

Abstract

Radio over fiber is becoming an increasingly important technology for the wireless market since it introduces a good data transmission rate and large bandwidth. We have demonstrated a bidirectional radio over fiber ROF system based on a reflective semiconductor optical amplifier (RSOA) utilizing an offset quadrature differential phase shift keying (OQPSK) signal for down-link and an on-off keying (OOK) signal re-modulated for up-link. We have performed a detailed comparison between OQPSK and DPSK according to the system behavior.

We have also implemented a combination of SCM-ROF and optical wavelength division multiplexing (WDM) techniques to simplify the access network architecture. The combination of two different types has been performed to provide high bit data rate and wide bandwidth in cellular communication. The system allows different Base Stations (BS's) to be fed by a common fiber. Different wavelength channels can be allocated to different BSs depending on user requirements.

We have also presented an investigation on the performance of Orthogonal Frequency Division Multiplexing (OFDM) system in terms of degradation of channel capacity, variation of optical input power and variation of number of subcarriers. OFDM is an attractive technique for achieving high bit rate data transmission.

Several measurements are found; the eye diagram, Bit Error Rate (BER) curves for both uplink and downlink, RSOA gain curve and noise figure with the variation of input power and temperature for each system.

ملخص الرسالة

تتزايد أهمية ارسال موجات الراديو عبر الألياف البصرية ROF بشكل ملحوظ في عالم الاتصالات نظرا لأنها تقدم سرعة نقل عالية للبيانات وتزود نطاق عرض البيانات، فمن هنا قمنا ببناء نظام ارسال ثنائي لموجات الراديو عبر الألياف الضوئية بالاعتماد علي المكبر العاكس الشبه موصل الضوئي RSOA وذلك باستخدام تقنية التضمين OQPSK لمرحلة التنزيل ومن ثم اعادة تضمين للموجة المرسله باستخدام OOK لمرحلة الارسال، كما وأجريت مقارنة تفصيلية بين تقنية OQPSK و DPSK من حيث كفاءة وأداء النظام.

كما وقمنا ببناء أنظمة ارسال مشابهة ولكن باستخدام تقنية مدمجة بين SCM و WDM حيث تستخدم هذه التقنية لتبسيط بنية الشبكة ، كما أنها تسمح بتغذية عدة محطات إرسال باستخدام كابل ضوئي مشترك ، كذلك تسمح بوجود عدة قنوات اتصال لكل محطة ارسال بحسب متطلبات المستخدم.

أيضا قمنا بفحص أداء نظام توزيع وتقسيم الترددات المتعامدة OFDM عبر نظام ارسال موجات الراديو من خلال الألياف الضوئية من حيث تدهور سعة قنوات الاتصال و تغيير القدرة المدخلة وكذلك بتغيير عدد الحوامل الفرعية ، هذا وتعتبر تقنية OFDM وسيلة ناجحة لتحقيق معدل نقل بيانات عالي السرعة.

ومن خلال الرسالة أوجدنا عدة علاقات مثل سعة العين و منحنيات نسبة الخطأ ومعامل تكبير RSOA ومعامل التشويش مع تغيير في درجات الحرارة أو القدرة المدخلة أو عدد قنوات الاتصال في كل نظام تم ذكره.

Acknowledgement

I would like to express my deepest gratitude for my parents who have always been there to support me. I also thank my wife who has been strongly supportive to me to the end of this thesis.

I am also greatly thankful to my supervisor, Dr. Fady El-Nahal, whose encouragement, guidance and support from the initial to the final phase enabled me to develop a deep and thorough understanding of the subject. Finally, I offer my regards and blessings to all of those who supported me in any respect during the completion of the thesis.

Mamoun Salha

Table of Contents

Abstract	II
ملخص الرسالة	III
Acknowledgement	IV
Table of Contents	V
List of Tables	IX
Abbreviations	X
Chapter 1 - Introduction	1
1.1 Thesis Statement	1
1.2 Background	1
1.3 Research Problem	2
1.4 Scope of Implementation	3
1.5 Literature Review.....	3
1.6 Thesis Structure.....	5
Chapter 2 – Preliminary Discussions	6
2.1 Radio over Fiber.....	6
2.2 Reflective Semiconductor Optical Amplifier (RSOA)	9
2.3 OFDM Technique	10
2.4. Phase-Shift Keying (BPSK).....	14
2.4.1 Binary phase-shift keying (BPSK).....	14
2.4.2 Quadrature phase-shift keying (QPSK).....	16
2.4.3 Differential phase-shift keying (DPSK).....	19
2.5 Subcarrier Multiplexing	20
Chapter 3 –System Analysis	22
3.1 System Model	22
3.2 QPSK modulation	24

3.3 Differential Phase Shift Keying (DPSK)	42
3.4 Subcarrier AM Modulation (SCM-AM)	45
3.5 Orthogonal Frequency Division Multiplexing (OFDM)	50
Chapter 4 –Conclusion	55
References	57

List of Figures

Figure 2- 1: ROF structure	6
Figure 2- 2:ROF categories.....	7
Figure 2- 3: OFDM implementation	11
Figure 2- 4:OFDM frequency spectrum.....	13
Figure 2- 5:Block diagram of OFDM modulation and demodulation.....	14
Figure 2- 6:Constellation diagram for BPSK.....	15
Figure 2- 7:Constellation diagram for QPSK with gray coding.....	17
Figure 2- 8:Conceptual transmitter structure for QPSK.....	18
Figure 2- 9:The structure of QPSK Receiver.....	18
Figure 2- 10:Sub-Carrier Multiplexing of broadband mixed mode data in RoF Systems.	20
Figure 3- 1:Schematic of a bidirectional RoF system	23
Figure 3- 2: OQPSK modulated signal.	24
Figure 3- 3: The MZM transmitted signal at 193.1 THz.....	26
Figure 3- 4:The electrical signal after PD	28
Figure 3- 5:The frequency domain representation of filtered signal after PD	28
Figure 3- 6:The plot of a band pass filtered OQPSK modulated signal in time domain.....	29
Figure 3- 7:The plot of a band pass filtered received signal in a (0-15ns) interval.....	29
Figure 3- 8:Quadrature demodulator block diagram.....	30
Figure 3- 9: Frequency spectrum of the demodulated signal.....	31
Figure 3- 10: The plot of a time domain demodulated signal.	31
Figure 3- 11:The block diagram of the internal connection of 3R regenerator.....	32
Figure 3- 12:The frequency spectrum of the recovered signal.....	33
Figure 3- 13:The reflected signal from RSOA.....	34

Figure 3- 14:Eye diagram of the downstream signal at input power of 10dBm.	35
Figure 3- 15:Eye diagram of the upstream signal at input power of 10dBm.	35
Figure 3- 16:BER versus input power at a fixed temperature (300 C).....	37
Figure 3- 17: The variation of RSOA gain with input power.	38
Figure 3- 18:The variation of the BER with temperature.	39
Figure 3- 19:The variation of the BER with temperature.	40
Figure 3- 20: The variation of the noise figure with temperature.	41
Figure 3- 21:Eye Diagram of DPSK down link stage.	42
Figure 3- 22:Eye Diagram of DPSK uplink stage.....	43
Figure 3- 23: BER curves of OQPSK and DPSK.	44
Figure 3- 24:RSOA gain vs. input power for OQPSK and DPSK.	45
Figure 3- 25:A bidirectional SCM-WDM RoF network.	46
Figure 3- 26:Eye Diagram of the downstream.	47
Figure 3- 27:Eye Diagram of the upstream.	48
Figure 3- 28:BER vs. input power for uplink and downlink.....	48
Figure 3- 29:Gain vs. input power at a fixed temperature.	49
Figure 3- 30:BER of SCM vs. number of channels at a fixed input power.	49
Figure 3- 31:Frequency domain presentation of OFDM signal.	51
Figure 3- 32:Frequency domain presentation of transmitted signal.....	51
Figure 3- 33:Eye diagram of the downlink stage.	52
Figure 3- 34:Eye diagram of the uplink stage.	53
Figure 3- 35:The variation of the BER with input power.	53
Figure 3- 36:The variation of the BER with number of subcarrier.	54

List of Tables

Table 3- 2: The CW laser parameter	25
Table 3- 3: Bidirectional optical fiber parameters	27
Table 3- 4: PD parameters.....	27
Table 3- 5: The parameters of the quadrature demodulator.	30
Table 3- 6 : PSK sequence decoder outputs.....	33
Table 3- 7: Eye diagram parameters comparison of the uplink stage and downlink stage	36
Table 3- 8 : PSK sequence decoder outputs.....	41

Abbreviations

AM	Amplitude Modulation
AWG	Arrayed Waveguide Grating
BER	Bit Error Rate
BPSK	Binary Phase Shift Keying
BS	Base Station
CATV	Cable Television
CDMA	Code Division Multiple Access
CO	Central Office
CW	Continuous Wave
DFT	Discrete Fourier Transformation
DPSK	Differential Phase Shift Keying
FFT	Fast Fourier Transformation
GSM	Global System for Mobile Communication
IF	Intermediate Frequency
IFFT	Inverse Fast Fourier Transformation
IM	Intensity Modulation
MCM	Multi Carrier Modulation
MSC	Mobile Switching Center
MVDS	Multipoint Video Distribution Services
MZM	Mach Zehnder Modulation
NF	Noise Figure
NRZ	Non Return Zero
OFDM	Orthogonal Frequency Multiple Access
OL	Optical Link
ONU	Optical Network Units
OOK	On Off Keying
OQPSK	Offset Quadrature Phase Shift Keying
OTDM	Optical Time Division Multiplexing
PD	Photo- Diode
PIN	P-type Intrinsic N-type
QAM	Quadrature Amplitude Modulation
QPSK	Quadrature Phase Shift Keying

RAP	Radio Access Point
RF	Radio Frequency
RoF	Radio over Fiber
RS	Remote Station
RSOA	Reflective Semiconductor Optical Amplifier
SCM	Sub Carrier Modulation
SMF	Single Mode Fiber
WDM	Wavelength Division Multiplexing
WLAN	Wireless LAN

This page left intentionally blank

Chapter 1 - Introduction

1.1 Thesis Statement

This thesis discusses the effective design of Radio over Fiber (RoF) system that can be integrated with several modulation types to model a new diagram of a bidirectional transmission ROF system using Reflective Semiconductor Optical Amplifier (RSOA) in downlink and uplink stages. Many modulation techniques have been used and parameters have been verified in each case. We simulate using the following types of modulation Offset Quadrature Phase Shift Keying (OQPSK), Differential Phase Shift Keying (DPSK), Quadrature Amplitude Modulation (QAM), Orthogonal Frequency Multiple Access (OFDM) and Subcarrier Modulation/ Wavelength Division Multiplexing SCM/WDM.

The main idea is to provide a large bandwidth to cover the huge data transferred between base stations and the central office with minimum cost effective system. This will enable the clients to enjoy multimedia services. The ideas presented in this thesis are the author's original works. The implementations and results are also accurate and were obtained solely by the author.

1.2 Background

RoF technology is a technology by which microwave (electrical) signals are distributed by means of optical components and techniques. A RoF system consists of a Central Site (CS) and a Remote Site (RS) connected by an optical fiber link or network. If the application area is in a GSM network, then the CS could be the Mobile Switching Centre (MSC) and the RS is the base station (BS). For wireless Local Area Networks (WLANs), the CS would be the head end while the Radio Access Point (RAP) would act as the RS [1].

In several studies of bidirectional systems, a reflective semiconductor optical amplifier (RSOA) operating as a modulator often plays an important role, and both the

upstream and down-stream channels use the same wavelength. This strategy is very useful for improving the wavelength utilization efficiency [2].

1.3 Research Problem

Internet communication services play an essential role in our life, and are considered as one of the universal communication platforms and rapidly becoming widely available that present mobile network users want to be able to use their mobile terminals and enjoy the same user experience as they do while connected to their fixed network either at work or at home . On other hand, wireless and mobile network technologies have witnessed a great development. Mobile phone penetration exceeds that of fixed phones in most developed countries. The proliferation of wireless devices coupled with increased demand for broadband services are putting pressure on wireless systems to increase capacity. So that wireless communications should enter a new phase to meet multimedia services [3]. To achieve this, wireless systems must have increased feeder network capacity, operate at higher carrier frequencies, and cope with increased user population densities. The raising of the carrier frequency would limit propagation characteristics; as a consequence, small cell sizes are formed. This leads to a large number of cells in a certain area, and then large number of remote antenna base stations (BSs) is required to cover an operational geographical area. These BSs provide wireless connectivity to users via millimeter-wave and are connected with a central office (CO) via an optical fiber access network. These leading to costly radio systems while the high installation and maintenance costs associated with high-bandwidth silica fiber render it economically impractical for in-home and office environments.

This thesis provides both Radio-Over-Fiber (RoF) technology and Reflective Semiconductor Optical Amplifier (RSOA) to emerge a cost effective approach for reducing radio system costs because it simplifies the remote antenna sites since RSOA work as an amplifier and modulator, the project also enhances the sharing of expensive radio equipment located at Central Sites (CS).

1.4 Scope of Implementation

The ideas in this thesis can be applied for many networks. The main purpose of the project is to provide more capacity and economic system. The use of RoF system integrated with RSOA reduces installation and maintenance costs while offering more capacity than the present copper-based infrastructure. Therefore, the proposed system has the potential to make high-density wireless systems of the future, economically and technically feasible.

The functionality of RoF application technology exceeds modulation and frequency conversion to include signal processing such as filtering and attenuation control at high frequencies which referred to as microwave functions. Many of these functions are difficult to achieve in the electrical domain due to limited bandwidth and other electromagnetic wave propagation limitations. However, if the processing is done in the optical domain, unlimited signal processing bandwidth becomes available. As a result, many microwave functions can be performed by optical components without needing E/O conversion for processing by microwave components and vice versa [4].

Some of the applications of RoF technology include cellular networks, satellite communications, broadband access radio, vehicle communications and control, Multipoint Video Distribution Services (MVDS), and wireless LANs over optical networks. The main advantages of RoF technology revolve in large bandwidth, low attenuation loss and immunity to interference [5].

1.5 Literature Review

Since the last decade, many millimeter wave band RoF systems have been studied. For initial deployment, a simple and low cost BS design is desirable. In addition, a variety of SCM / WDM RoF systems have been studied to increase the channel capacity in existing optical fibers.

Fady I. El-Nahal built up a bidirectional subcarrier modulation-wavelength division multiplexing (SCM-WDM) RoF network using a reflective semiconductor optical amplifier (RSOA) and cyclic arrayed waveguide gratings (AWGs). The purposed RoF network utilizes Sub Carrier Multiplexed (SCM) signals for down-link and an on-off

keying (OOK) signals re-modulated for up-link. In this paper, A 50 km range colorless WDM-ROF was demonstrated for both 1 G bit/s downstream and upstream signals [6].

Xianbin Yu, T. B. Gibbon, and I. T. Monroy demonstrated a bidirectional radio-over-fiber (RoF) system based on a reflective semiconductor optical amplifier (RSOA) where phase-modulated 5.25-GHz radio frequency (RF) carrying 850 Mb/s is used for the downstream signal. Optical envelope detection of 10-GHz RF carrying 850 Mb/s was achieved in an RSOA. Moreover, there is no need to employ RF down-conversion technology for RoF uplink. This makes the proposed system simpler and more cost-effective. The experimental results indicate that after simultaneous transmission of downstream and upstream signals over 25-km fiber, the receiver sensitivities are 22 and 14.5 dBm, respectively [7].

M.C.R. Medeiros proposed the RoF net-Reconfigurable Radio over Fiber network which combines a low cost Base Station (BS) design, incorporating reflective semiconductor optical amplifiers (RSOA), with fiber dispersion mitigation provided by optical single sideband modulation techniques. Optical wavelength division multiplexing (WDM) techniques are used to simplify the access network architecture allowing for different Base Stations to be fed by a common fiber [8].

M. Arief, Sevia M. Idrus and S. Alifah investigated a subcarrier (SCM) system integrated with WDM system with various issues in order to provide a cost-effective, high performance solution for high speed data rates by the available bandwidth of the electrical and optical components. The results are presented higher bandwidth for long distance communication system (SMF, 150 km) by using SCM/WDM for Radio over Fiber. Therefore, the efficiency of bandwidth utilization of SCM is expected to be much better than conventional optical WDM [9].

N. Mohamed, S.M. Idrus introduced mm-wave carrier generation techniques for radio over fiber including: optical heterodyning, external modulation, optical transceiver, and up-and down-conversion [10].

Cristina Arellano and Carlos Bock presented designs of low cost optical network units (ONU) for wavelength division multiplexing-passive optical networks (WDM-PON). Reflective SOAs are proposed to be used as core of the ONU in a bidirectional single-fiber

single-wavelength topology. Forward Error Correction (FEC) is employed to mitigate crosstalk effects. The results showed that The FSK-ASK system have better performance in terms of sensitivity and bit rate, while full-duplex transmission is offered [11].

Capmany et al. suggested assembling optical de-multiplexing in a system, where both WDM and SCM technologies were combined [12].

Jianping Wang, Xianwei Zhou, and Wen Wang are built up a radio-over-fiber (ROF) network based on the orthogonal frequency division multiplexing (OFDM) system simulation model. Special attention had been paid on the high peak-to-average power ratio (PAPR) of the OFDM signal which greatly constrained the performance of the OFDM-ROF system. A clipping and filtering technology had been investigated and simulated. Compared with the Naquist sampled, the two over sampled signal had a better performance in reducing PAPR. The bit error rate (BER) error flow research had been done with transmitting the clipped signal in nonlinear distorted ROF link. And the QAM had been testified for the preferred technique in OFDM-ROF link [13].

1.6 Thesis Structure

This is written to bring the reader step by step going in the main core of the content. Chapter 1 Provides the introduction to this thesis where brief background of the study problem and to the statement of the problem, followed by the objective and the scope of the study.

Chapter 2 reviews the literature, which includes introduction to the RoF, the benefits, and applications of the radio over fiber technology in communication fields. In addition various types of modulations also have been covered.

Chapter 3 describes the methodological processes by showing detailed diagram of the methods implemented as well as highlighting briefly the steps those have been followed to achieve the objective of this project. Also, it presents the results derived from the methods explained where some analyses and simulations were done based on several effects.

Finally; Chapter 4 introduces the conclusions of the study, as well as some suggestions for future work.

Chapter 2 – Preliminary Discussions

In this chapter, we review the basic concepts behind this thesis. Mainly speaking, we will discuss the concepts of Radio over Fiber technology (RoF), the Reflective Semiconductor Optical Amplifier (RSOA), Orthogonal Frequency Division Multiplexing (OFDM) technique and other modulation and multiplexing types. For each concept, a quick and comprehensive review will be made. This includes the main concepts, the advantages, and the types available that distinguishes their usage in practice.

2.1 Radio over Fiber

2.1.1 Basic Concept

Radio over Fiber (RoF) is a technology that modulates the light wave with a radio signal directly without any electrical / optical conversions using optical components. Although radio transmission over fiber is used for multiple purposes, such as in Cable Television (CATV) networks and in satellite base stations [8].

Any RoF system in a simple structure consists of three main parts

- Central Office (CO).
- Remote Site (RS).
- Optical Link (OL).



Figure 2-1: ROF structure.

There are three main RoF transmission categories (Baseband-RoF, RF-RoF and IF-RoF) according to the frequency range of the radio signal to be transported; Figure 2-2 illustrates the three categories [14].

a) In baseband-RoF, a message data signal is used to modulate the light wave to transfer through the optical link. In other word, the message signal is the modulating signal and the light wave is the carrier signal.

b) In RF-RoF, a Radio Frequency signal with a high frequency is modulated with an optical light wave signal before being transported over the optical link. Therefore, wireless signals (RF signal) are optically distributed to base stations directly at high frequencies and there is no need to any up/ down conversions, thereby a less cost system is obtained.

c) In IF-RoF, an Intermediate Frequency radio signal with a lower frequency is used for modulating light before being transported over the optical link. Therefore, wireless signals are transported at intermediate frequency over the optical [5].

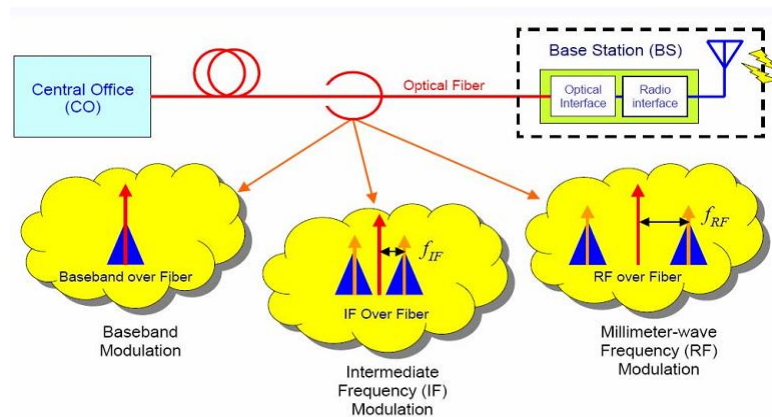


Figure 2- 2:RoF categories

2.1.2 RoF Benefits

Low attenuation loss

The attenuation loss occurred to the signal during its travel through the fiber is much lower than other mediums. In free space, distortion occurs due to reflections and absorptions which is increased with high frequencies; therefore electrical transmission to mm-wave is costly and not recommended for long distances. Commercially available standard Single Mode Fibers (SMFs) made from glass (silica) have attenuation losses below 0.2 dB/km and 0.5 dB/km in the 1.5 μm and the 1.3 μm windows, respectively. So by using optical fiber, the signal travels further reducing the need of repeaters [3].

Large Bandwidth

ROF technology introduces a huge bandwidth to meet the new technology multimedia applications; the combined bandwidth of the three windows is in the excess of 50 THz but the actually the commercial system utilize only 1.6 THz according to electronic hardware limitations. The advanced multiplexing techniques namely Optical Time Division Multiplexing (OTDM) in combination with Dense Wavelength Division Multiplex (DWDM) techniques is used to exploit more optical capacity [14].

Lower Cost

Most ROF techniques eliminate the need for a local oscillator and related equipment at the Remote Station (RS). Simpler structure of remote base station means lower cost of infrastructure, lower power consumption by devices and simpler maintenance, all of these contribute to lower the overall installation and maintenance cost [5] .

2.1.3 Millimeter Waves

Millimeter waves or mm-waves are considered as an "electronic bottleneck" since mm waves cannot be distributed electrically due to high RF propagation losses. In addition to the challenges of mm-wave frequencies generating using electrical devices. The most suitable solution to the problem is to use optical means. Low attenuation loss and large bandwidth make the distribution of mm-waves cost effective. Furthermore, some optical based techniques have the ability to generate unlimited frequencies. For instance, microwave frequencies that can be generated by Remote Heterodyning and Detection (RHD) methods are limited only by the bandwidth of photo detectors.

Millimeter waves provide high bandwidth due to the high frequency carriers. Also, in free space RF propagation losses are high, and hence propagation distances are severely limited. As a consequence, well-defined small radio sizes (micro- and pico cells) are formed; this leads to a considerable frequency re-use so that services can be delivered simultaneously to a larger number of subscribers [15].

The main disadvantage of mm-waves is the need for large number of BSs, which is a consequence of high RF propagation losses. Unless the BSs are simple enough, installing and maintaining the mm-wave system can be economically prohibitive owing to the numerous number of the required BSs.

2.2 Reflective Semiconductor Optical Amplifier (RSOA)

The RSOA can be used as an amplifier. This gives additional gain enabling the possibility of avoiding the use of an Erbium Doped Fiber Amplifier (EDFA) in the system. It is not as known, however, due to its properties it allows higher gain than the SOA and its gain nonlinearity is also interesting for wavelength conversion. Reflective semiconductor optical amplifier offers highly optimized performance for WDM Passive Optical Network (PON) applications. It capable of delivering 20 dB of gain, the semiconductor optical amplifier (SOA) can be modulated at rates up to 1.5 GB/s to provide wavelength-agile optical data transmission facilities for clients in fiber-to-the-home/premises (FTTH/FTTP) access network architectures - without the expense of a tunable wavelength source [16].

The RSOA is a cost-effective since it performs the functions of not only modulator (no need for local laser source), but also amplifier. It considers the possibility of sensing the differences in voltage produced at the bias electrode of the single-section SOA. The value of the injection current in the RSOA is considered as an input signal allowing the modulation of the optical signal by the SOA

$$\Psi_{\phi} = \eta_j \frac{K_B T}{c} \ln \left[\frac{N_{bias}(z) + N(z)}{N_{bias}(z)} \right] \quad (2.1)$$

Where:

Ψ_{ϕ} : Voltage variation.

η_j : Reflective coefficient.

K_B : Boltzmann constant.

T : RSOA Temperature

c : Light speed

$N_{bias}(z)$: Bias current level.

$N(z)$: Current level.

The Drawback of the RSOA setup was the stability with the polarization, since little movements in the fibers that connect the RSOA to the circulator resulted in a quite significant

2.3 OFDM Technique

Orthogonal frequency division multiplexing (OFDM) is a modulation technique which is now used in most new and emerging broadband wired and wireless communication systems because it is an effective solution to inter symbol interference caused by a dispersive channel. Very recently number of researchers have shown that OFDM is also a promising technology for optical communications.

2.3.1 Principles of orthogonal frequency-division multiplexing (OFDM)

OFDM is a special form of a broader class of multi-carrier modulation (MCM); it involves sending several signals at one given time over several different frequency channels, or subcarriers.

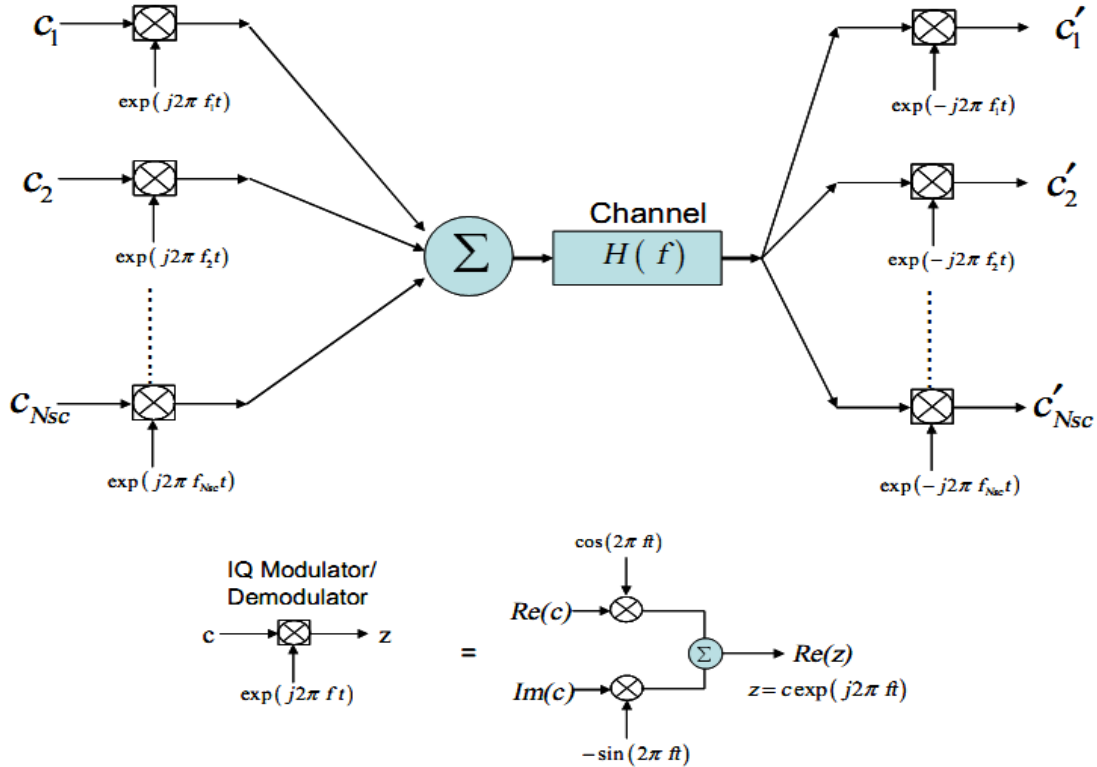


Figure 2- 3: OFDM implementation.

The structure of a complex mixer (IQ modulator/demodulator), which is commonly used in MCM systems, is shown in Figure 2-3 [17].

The MCM transmitted signal $S(t)$ is represented as:

$$\sum_{i=-\infty}^{+\infty} \sum_{k=1}^{N_{sc}} C_{ki} S_k(t - iT_s), \quad (2.2)$$

$$S_k(t) = \Pi(t) \exp(j2\pi f_k t), \quad (2.3)$$

$$\Pi(t) = \left\{ \begin{array}{l} 1, (0 < t \leq T_s) \\ 0, (t \leq 0, t > T_s) \end{array} \right\}, \quad (2.4)$$

where C_{ki} is the i_{th} information symbol at the k_{th} subcarrier, S_k is the waveform for the k_{th} subcarrier, N_{SC} is the number of subcarriers, f_k is the frequency of the subcarrier, and T_s is the symbol period. The optimum detector for each subcarrier could use a filter that matches the subcarrier waveform, or a correlator matched to the subcarrier as shown in Figure 2-3. Therefore, the detected information symbol C_{ik} at the output of the correlator is given by:

$$C_{ki} = \int_0^{T_s} r(t - iT_s) s_k^* dt = \int_0^{T_s} r(t - iT_s) e^{-j2\pi f_k t} dt \quad (2.5)$$

where $r(t)$ is the received time-domain signal. The classical MCM uses non-overlapped band-limited signals, and can be implemented with a bank of large number of oscillators and filters at both transmit and receive end. The major disadvantage of MCM is the required excessive bandwidth and the cost-efficiently which due to the design of filters and oscillators. On other hand, the channel spacing has to be multiple of the symbol rate, greatly reducing the spectral efficiency [18].

So that, to overcome this problem the OFDM technique is used. The main advantage of OFDM with respect to MCM is that the signals are orthogonal. Equation (2.6) and equation (2.7) explain the principle of orthogonality

$$\delta_{kl} = \frac{1}{T_s} \int_0^{T_s} s_k s_l^* dt = \frac{1}{T_s} \int_0^{T_s} \exp(j2\pi(f_k - f_l)t) dt \quad (2.6)$$

$$\delta_{kl} = \exp(j\pi(f_k - f_l)T_s) \frac{\sin(\pi(f_k - f_l)T_s)}{\pi(f_k - f_l)T_s} \quad (2.7)$$

Then to confirm the orthogonality, the following condition $(f_k - f_l) = \frac{m}{T_s}$ should be satisfied, the principle of orthogonality helps to ensure that cross talk does not occur between the carrier frequencies as shown in Figure 2-4 [19].

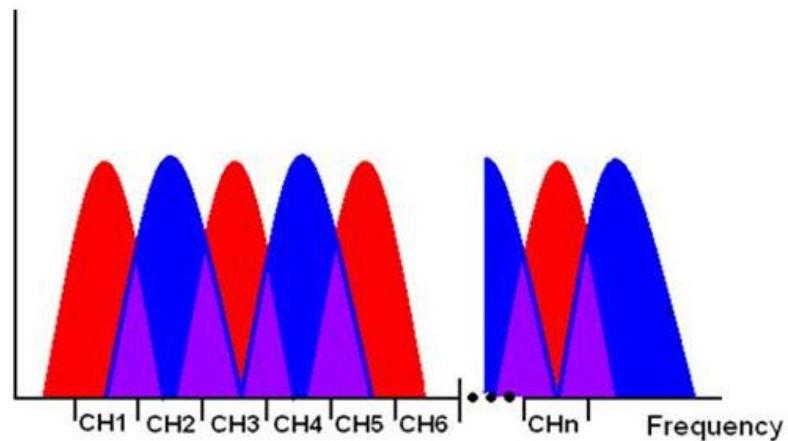


Figure 2- 4:OFDM Frequency Spectrum.

Despite the fact that the signals overlap in the frequency domain, it is possible, from a receiver's point of view, to extract data from one specific carrier simply by knowing its frequency.

2.3.2 OFDM Modulation and Demodulation

Weinstein and Ebert were first to reveal that OFDM modulation/demodulation can be implemented by using Inverse Discrete Fourier Transform (IDFT)/Discrete Fourier Transform (DFT). This is evident by studying OFDM modulation and OFDM demodulation. It follows that the modulation can be performed by IDFT of the input information as shown in Figure 2-5 [20].

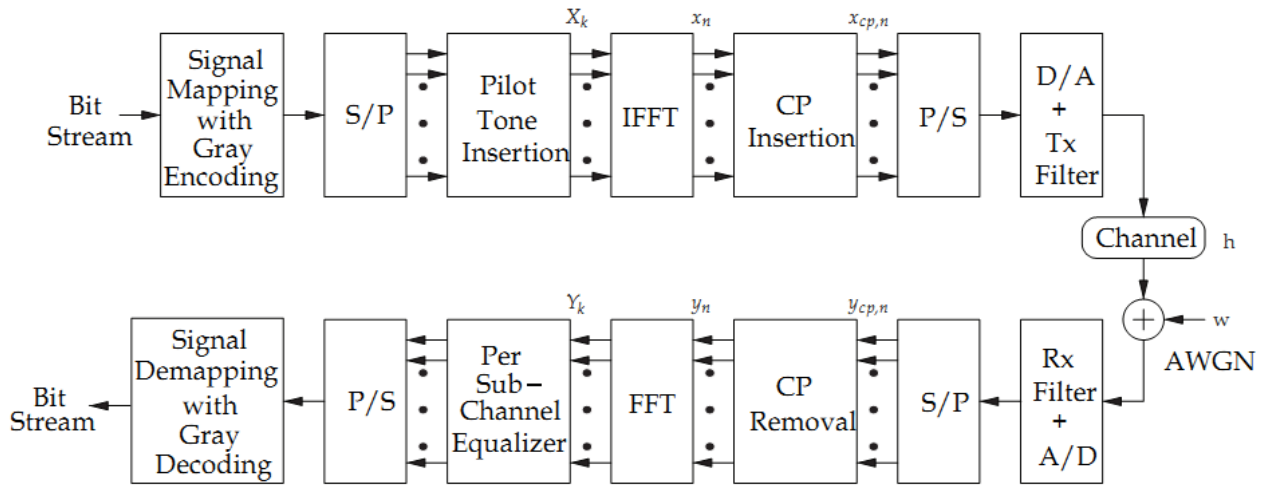


Figure 2- 5:Block diagram of OFDM modulation and demodulation.

The serial data stream is mapped to symbols with a symbol rate of $1/T_s$ using modulation scheme like M-PSK, QAM. The resulting symbol stream is de-multiplexed into N data symbols S_0 to S_{N-1} . The parallel data symbol rate is $1/NT_s$. This means the parallel symbol duration is N times longer than the serial symbol duration T_s . The inverse FFT (IFFT) of the data symbol is computed and the output S_0 to S_{N-1} constitutes an OFDM symbol. This symbol period is transmitted serially over the channel with symbol rate of $1/T_s$ after cyclic prefix insertion.

At the receiver, the received time domain symbols are decomposed by employing FFT operation, the recovered data symbols are restored in serial order.

2.4. Phase-Shift Keying (BPSK)

2.4.1 Binary phase-shift keying (BPSK)

One of the simplest forms of phase shift keying (PSK) is the binary phase shift keying BPSK. It uses two phases which are separated by 180° and so it is termed 2-PSK. It does not particularly matter exactly where the constellation points are positioned, they are shown on the real axis at 0° and 180° in Figure 2-6 [21].

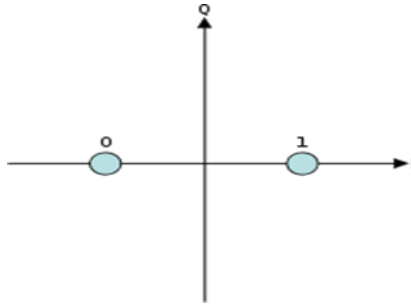


Figure 2- 6:Constellation diagram for BPSK.

The distance of the two symbols is a maximum distance and it takes the highest level of noise or distortion to make the demodulator reach an incorrect decision. In the case of a limited bandwidth; it is, however, unsuitable for high data-rate applications since it is only able to modulate at 1 bit/symbol. In the presence of an arbitrary phase-shift introduced by the communications channel, the demodulator is unable to tell which constellation point is which. As a result, the data is often differentially encoded prior to modulation. The general form for BPSK follows the equation:

$$S_n(t) = \sqrt{\frac{2E_b}{T_b}} \cos(2\pi f_c t + \pi(1-n)), n = 0,1. \quad (2.8)$$

Where

E_b : The bit energy.

T_b : Bit period.

f_c : Carrier frequency.

This yields two phases, 0 and π . In the specific form, binary data is often conveyed with the following signals:

$$S_0(t) = \sqrt{\frac{2E_b}{T_b}} \cos(2\pi f_c t + \pi) = -\sqrt{\frac{2E_b}{T_b}} \cos(2\pi f_c t) \quad (2.9)$$

$$S_1(t) = \sqrt{\frac{2E_b}{T_b}} \cos(2\pi f_c t) \quad (2.10)$$

Hence, the signal-space can be represented by the single basis function

$$\Phi(t) = \sqrt{\frac{2}{T_b}} \cos(2\pi f_c t) \quad (2.11)$$

The bit error rate (BER) of BPSK in AWGN is given by:

$$P_b = Q\left(\sqrt{\frac{2E_b}{N_0}}\right) \quad (2.12)$$

Since there is only one bit per symbol, this is also the symbol error rate [22].

2.4.2 Quadrature phase-shift keying (QPSK)

It is known as quaternary PSK, quadriphase PSK, 4-PSK, or 4-QAM. It uses four points on the constellation diagram, equispaced around a circle. With four phases, QPSK can encode two bits per symbol, with gray coding to minimize the bit error rate (BER) as shown in Figure 2-7. QPSK can be used either to double the data rate compared with a BPSK system while maintaining the same bandwidth of the signal, or to maintain the data-rate of BPSK but halving the bandwidth needed. In the second case, the BER of QPSK is exactly the same as the BER of BPSK, so the advantage of QPSK over BPSK becomes evident [22]. The general form of QPSK (This implementation is also used for higher-order PSK forms) is given by:

$$S_n(t) = \sqrt{\frac{2E_s}{T_s}} \cos\left(2\pi f_c t + (2n-1)\frac{\pi}{4}\right), n = 1, 2, 3, 4. \quad (2.13)$$

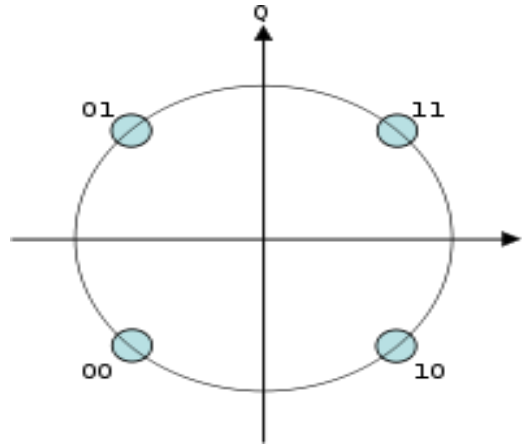


Figure 2- 7:Constellation diagram for QPSK with Gray coding.

This results in a two-dimensional signal space with the unit basis functions

$$\Phi_1 = \sqrt{\frac{2}{T_s}} \cos(2\pi f_c t), \Phi_2 = \sqrt{\frac{2}{T_s}} \sin(2\pi f_c t) \quad (2.14)$$

The first basis function is used as the in-phase component of the signal and the second as the quadrature component of the signal. Hence, the signal constellation consists of the

signal-space 4 points $\left(\pm\sqrt{\frac{E_s}{2}}, \pm\sqrt{\frac{E_s}{2}} \right)$.

The factors of 1/2 indicate that the total power is split equally between the two carriers. QPSK systems can be implemented in a number of ways . An illustration of the major components of the transmitter and receiver structure are shown in Figure 2-8 and Figure 2-9 respectively [21].

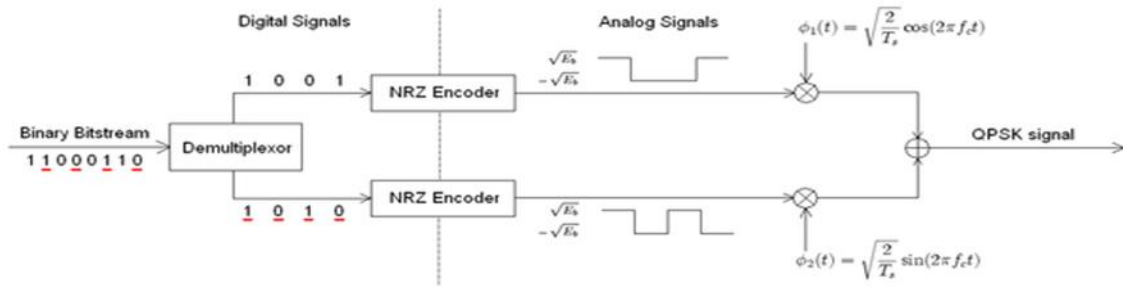


Figure 2- 8: Conceptual transmitter structure for QPSK.

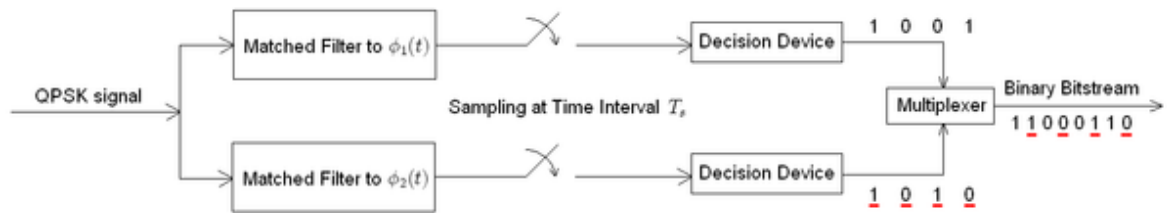


Figure 2- 9: The structure of QPSK Receiver.

The matched filters can be replaced with correlators. Each detection device uses a reference threshold value to determine whether a 1 or 0 is detected, the probability of bit error for QPSK is the same as for BPSK:

$$P_b = Q\left(\sqrt{\frac{2E_b}{N_o}}\right) \quad (2.15)$$

However, in order to achieve the same bit-error probability as BPSK, QPSK uses twice the symbol power (since two bits are transmitted simultaneously). The symbol error rate is given by:

$$P_s = 1 - (1 - P_b)^2 \quad (2.16)$$

$$= 2Q\left(\sqrt{\frac{E_s}{N_o}}\right) - Q^2\left(\sqrt{\frac{E_s}{N_o}}\right) \quad (2.17)$$

If the signal-to-noise ratio is high (as it is necessary for practical QPSK systems) the probability of symbol error may be approximated:

$$P_s \approx 2Q \left(\sqrt{\frac{E_s}{N_o}} \right) \quad (2.18)$$

2.4.3 Differential phase-shift keying (DPSK)

Differential phase shift keying (DPSK) is a common form of phase modulation that conveys data by changing the phase of the carrier wave. In differentially-encoded QPSK (DQPSK), the phase-shifts are 0° , 90° , 180° , -90° corresponding to data '00', '01', '11', '10'. This kind of encoding may be demodulated in the same way as for non-differential PSK but the phase ambiguities can be ignored.

In both BPSK and QPSK, there are phase ambiguity problems at the receiving end, this problem can be overcome by using the data to change rather than set the phase, so differentially encoded QPSK and BPSK is often used in practice. Analysis shows that differential encoding approximately doubles the error rate compared to ordinary M-PSK but this may be overcome by only a small increase in E_b / N_o . Furthermore, there will also be a physical channel between the transmitter and receiver in the communication system. This channel, in general, will introduce an unknown phase-shift to the PSK signal; in these cases the differential schemes can yield a better error-rate than the ordinary schemes which rely on precise phase information [23].

In optical communications, the data can be modulated onto the phase of a laser in a differential way. For the case of BPSK for example, the laser transmits the field unchanged for binary '1', and with reverse polarity for '0'. The demodulator consists of a delay line interferometer which delays one bit, so two bits can be compared at one time. In further processing, a photodiode is used to transform the optical field into an electric current, so the information is changed back into its original state.

2.5 Subcarrier Multiplexing

Subcarrier Multiplexing (SCM) is multiple radio frequency (RF) carrying signals to transmit through optical fiber using single wavelength. It is a maturing simple and cost effective approach for exploiting optical fiber bandwidth in RoF systems in particular [9].

In SCM, a microwave signal (the subcarrier) is used to modulate an optical carrier at the transmitter's side. This results in an optical spectrum consisting of the original optical carrier f_0 , plus two side-tones located at $f_0 - f_{sc}$ and $f_0 + f_{sc}$ where f_{sc} is the subcarrier frequency. If the subcarrier itself is modulated with data (analogue or digital), then sidebands centered on $f_0 - f_{sc}$ and $f_0 + f_{sc}$. To multiplex multiple channels on one optical carrier, multiple subcarriers are first combined and then used to modulate the optical carrier. At the receiver's side the subcarriers are recovered through direct detection and then radiated, different modulation schemes may be used on the different subcarriers. In addition, the data used to modulate the subcarriers need not be of the same kind [14].

One subcarrier may carry digital data, while another may be modulated with an analogue signal such as video or telephone traffic. In this way, SCM supports the multiplexing of various kinds of mixed mode broadband data as shown in Figure 2-10 [24].

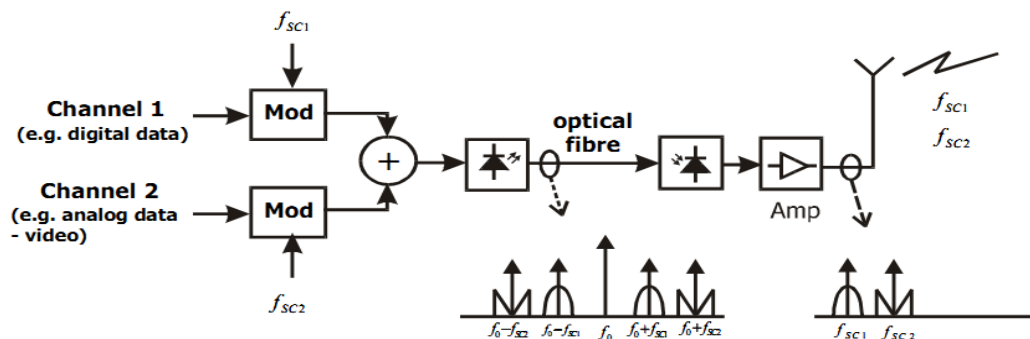


Figure 2- 10:Sub-Carrier multiplexing of broadband mixed mode data in RoF Systems.

According to the fact that the modulation technique used and data carried on each subcarrier are independent of what happens on other subcarriers, then SCM supports mixed mode data traffic. Therefore, it can be used for a wide range of applications such as

CATV, and wireless LANs. Furthermore, because the subcarriers are low frequencies, components required for SCM-based systems are readily available. Modulators, mixers and amplifiers employed in cable (or community) TV (CATV) and other satellite systems can still be used in SCM systems leading to low system costs.

The disadvantage of SCM is that being an analogue communication technique, it is more sensitive to noise effects and distortions. This places stringent linearity requirements on the performance of components especially for applications such video, where a Carrier-to- Noise-Ratio (CNR) > 55 dB may be required [25].

Chapter 3 –System Analysis

In this chapter, we review the implementation details of a bidirectional radio over fiber system architecture. The chapter first describes the proposed system model, explains the implementation environment and then the final results are summarized. The chapter also compares main measurements and system efficiency of each modulation type.

3.1 System Model

In this chapter, we discuss the main parts of the system model and their functionalities which are modulator, Arrayed Waveguide Grating (AWG), RoF link, demodulators and the RSOA. The proposed RoF architecture is shown in Figure 3-1. For down-link, a series of Continuous Wave (CW) lasers with various wavelengths are modulated by phase modulators using 1 Gb/s non-return to zero (NRZ) downstream data to generate the desired downstream signal. The generated signal is sent over the bidirectional Single-Mode Fiber (SMF). A circulator is used in the central office (CO) to separate the downstream and upstream traffic. The modulated signals are sent to Optical Network Unit (ONU). At the ONU, using optical splitter/coupler, portion of the modulated signal is fed to a balanced receiver. For up-link, the other portion of the downstream modulated signal from the splitter/coupler is re-modulated using 1 Gb/s NRZ upstream data by RSOA in the ONU. The re-modulated OOK signals re-pass through the bidirectional SMF and get to the bidirectional AWG. By using the circulator to avoid influencing the downstream signals, the upstream signals are sent to a P-type Intrinsic N-type (PIN) receiver is used to receive the upstream signal in the CO.

The system model is categorized into three main parts which are Central Office (CO), single mode fiber channel, Remote Station (RS) or Base Station (BS). The main components used in the system are as follows:

PRBS: Generates a Pseudo Random Binary Sequence (PRBS) according to different operation modes. The bit sequence is designed to approximate the characteristics of random data.

PSK: Encodes and modulates a binary signal to an electrical signal using phase shift keying modulation (PSK).

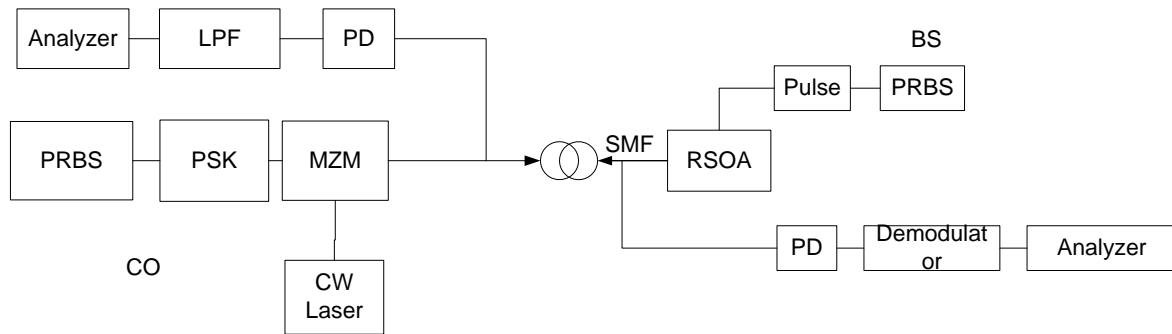


Figure 3- 1:Schematic of a bidirectional RoF system

MZM: The Mach-Zehnder modulator is an intensity modulator based on an interferometry principle. It consists of two 3 dB couplers which are connected by two waveguides of equal length. By means of an electro-optic effect, an externally applied voltage can be used to vary the refractive indices in the waveguide branches. The different paths can lead to constructive and destructive interference at the output, depending on the applied voltage. Then the output intensity can be modulated according to the voltage.

AWG: Arrayed Waveguide Grating (AWG) is an optical device based on interferential phenomena, and it has a periodic behavior in the wavelength domain. The input optical signals in each port are routed to a specific output port depending on the signal wavelength and the input port number.

PD: The incoming optical signal and noise are filtered by an ideal rectangle filter to reduce the number of samples in the electrical signal. The new sample rate is defined by the parameter sample rate. You can define the center frequency, or it can be calculated automatically by centering the filter at the optical channel with maximum power.

Bidirectional SMF: The component simulates the bidirectional propagation of arbitrary configuration of optical signals in a single-mode fiber. Dispersive and nonlinear – Self Phase Modulation (SPM), Cross Phase Modulation (XPM), Stimulated Raman (SRS) and Brillouin (SBS) scattering effects are taken into account. Raman interaction for an arbitrary configuration of sampled and parameterized signals is also considered. The component provides most of the functionality of the total field approach fiber model.

RSOA: simulates a reflective semiconductor optical amplifier including the dynamic dependence between electric and optical input signals.

3.2 OQPSK modulation

3.2.1 Transmitter Stage

The input data of the system is a pseudo random bit sequence at 1 G bps bit rate and it is directly modulated using OQPSK modulator at a frequency equals 2 GHz with normalized signal amplitude and 45° phase offset with 0 DC biasing. Table 3-1 summarizes the parameters of the OQPSK modulator.

Parameter	Value
Frequency	2 GHz
Amplitude	1 a.u.
Bias	0
Phase offset	45 degree

Table 3- 1: OQPSK modulator parameter.

The OQPSK modulated signal is illustrated in Figure 3-2, the central frequency of the signal is 2 GHz with 2 GHz major bandwidth from 1 GHz to 3 GHz in two sidebands.

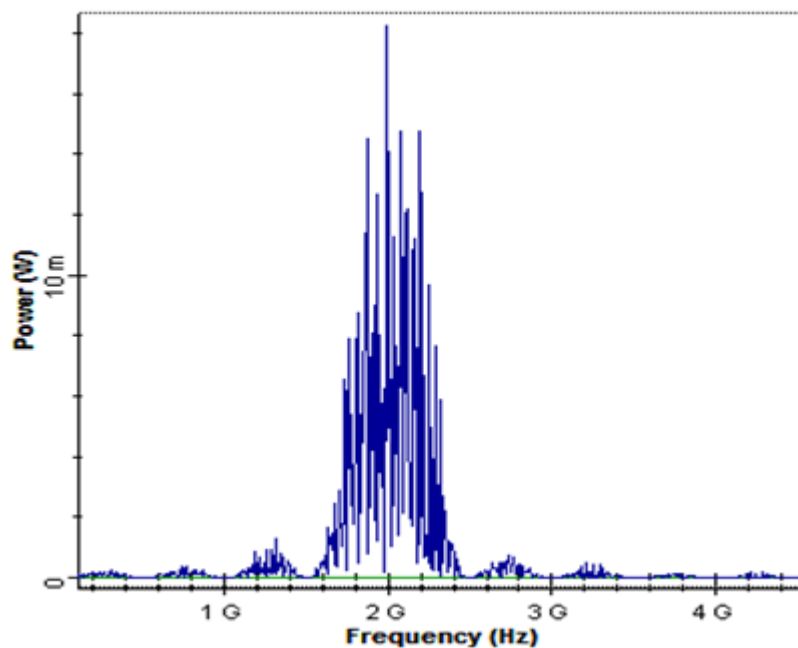


Figure 3- 2: OQPSK modulated signal.

The parameters of CW laser are configured as shown in Table 3-2. Frequency indicates the central frequency of the laser and determines the wavelength of the emitted light wave. Average power specifies the power of output light wave. Line width characterizes the width of the frequency interval of the total emission area. Initial phase gives the initial phase of oscillation to generate wave light.

Parameter	Value
Frequency	193.1 THz
Power	(0-12) dBm
Line width	10 MHz
Initial Phase	0 degree

Table 3- 2: The CW laser parameter

The Mach Zehnder Modulator has three ports: the first port is for electrical modulation type, the second is the CW laser input and the third port is the outlet of output optical signal. The extinction ratio is set to 30 dB to characterize the division power ratio of the upper path to lower path. The output optical signal is shown in Figure 3-3. It is clear from the figure that there is symmetry about 193.1 THz. The output power is measured by using the optical power meter before and after the circulator; $P_{out (Before)} = 8.99 \text{ dBm}$ and $P_{out (After)} = 7.99 \text{ dBm}$, the power loss is due to the insertion loss of the circulator.

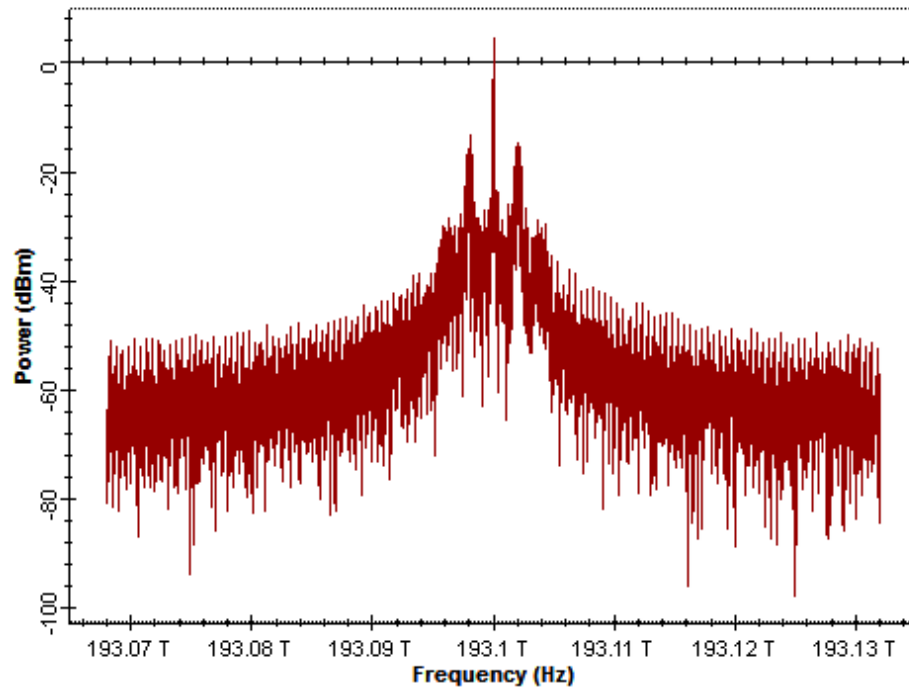


Figure 3- 3: The MZM transmitted signal at 193.1 THz.

3.2.2 Channel Stage

A bidirectional single mode fiber of 50 km is used to forward the signal and to backward it with an optical delay of 1 unit in order to separate the upstream and downstream. Table 3-3 shows the main parameters of a bidirectional optical fiber.

The fiber cable has an attenuation loss of 0.22 dB/km and length of 50 km, this means there is a $0.22 \text{ dB/km} \times 50 \text{ km}$ which equal to 11 dB power loss, so that the resultant signal power is equal to $7.99 \text{ dBm} - 11 \text{ dB} = -3.01 \text{ dBm}$ (Theoretical Analysis).

On other hand, the measured signal power after travelling through the optical fiber cable is equal to -3.01 dBm, so that there is a matching between theoretical analysis and simulated measurements.

Parameter	Value
Reference wavelength	1550 nm
Length	50 km
Attenuation	0.22 dB/km
Dispersion	16.75 ps/nm/km
Dispersion slope	0.075 ps/nm ² /km

Table 3- 3:Bidirectional optical fiber parameters

The signal passes the optical fiber to another circulator which also has 1dB insertion loss and so the resultant power signal decreases 1 dBm to become -4 dBm, then the signal is distributed into two paths the first towards RSOA branch and the second towards downlink stage receiver. First; we will continue in downlink stage and hence, analysis the RSOA and uplink stage.

3.2.3 Downlink Receiver Stage

The optical signal is received by photodetector PD operating at 193.1 THz frequency to convert it back to electrical form, the received signal after photo detection is illustrated in Figure 3-4. It is clear that the central frequency of the signal is about 2 GHz with major bandwidth equal to 12 GHz; also it is clear that there is a power loss and signal distortion due to conversion process in spite of using sampling rate in PD five times of the main sampling rate, the signal power decreases to -42.775 dBm.

To recover the message signal; a band pass Bessel filter BPF is used with central frequency of 2 GHz and 0.8 GHz bandwidth, the filter order is 8 to increase the sharpness of filter edges and to decrease the transition area, more BPF parameters are included in Table 3-4.

Parameter	Value
Frequency	2 GHz
Bandwidth	0.8 GHz
Insertion loss	2 dB
Depth	100 dB
Order	8

Table 3-4:PD parameters

The resultant signal power after the BPF is about -49.84 dBm, the power losses is due to the signal cutting; the output electrical signal is shown in Figure 3-5.

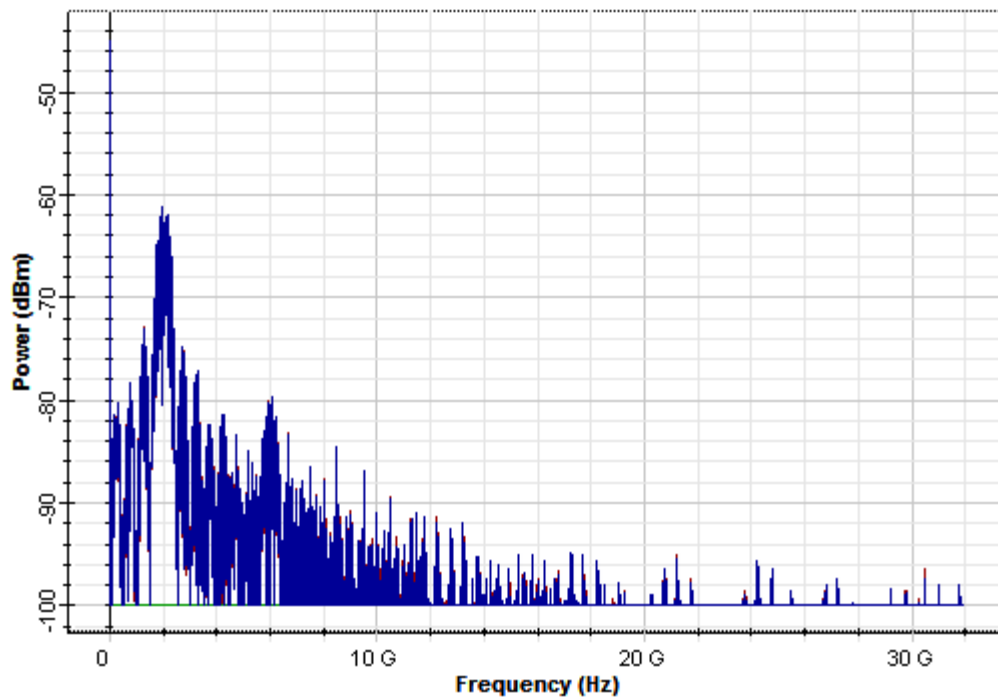


Figure 3- 4:The electrical signal after PD.

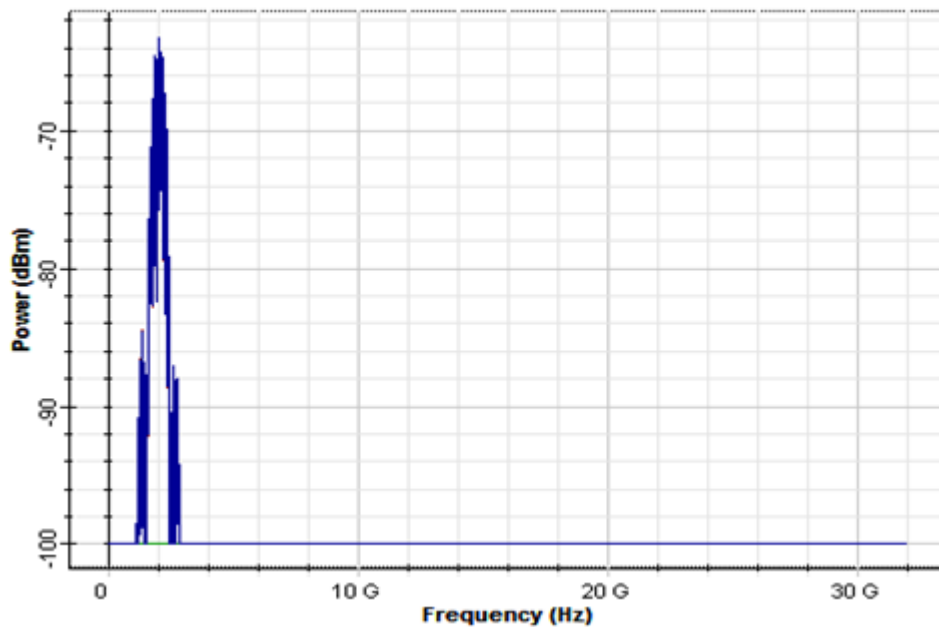


Figure 3- 5:The frequency domain representation of filtered signal after PD.

The plot of a time domain band pass microwave filtered signal at 2 GHz carrier frequency carrying OQPSK modulated data is shown in Figure 3-6.

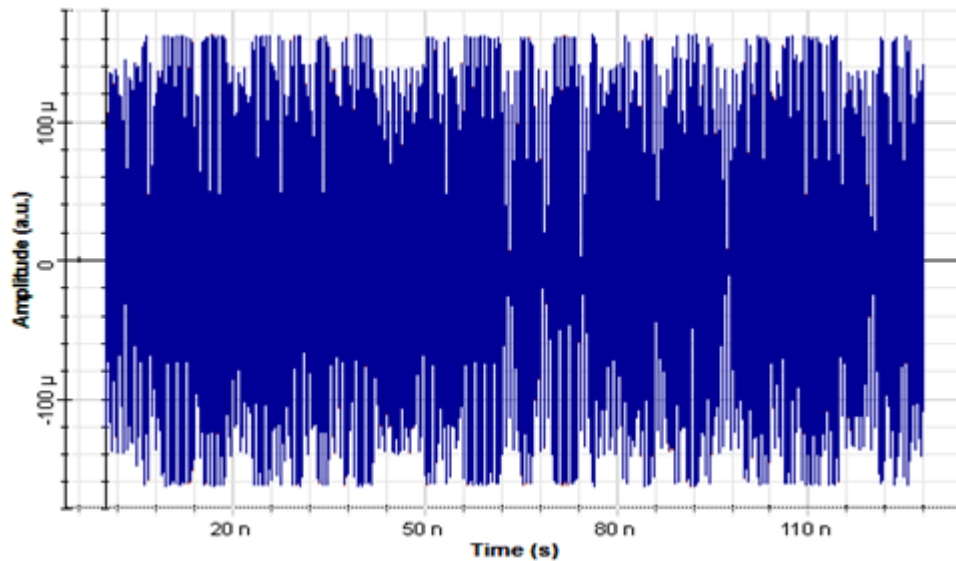


Figure 3- 6: The plot of a band pass filtered OQPSK modulated signal in time domain.

For more illustration; a certain interval from 0 ns to 15 ns is chosen in Figure 3-7

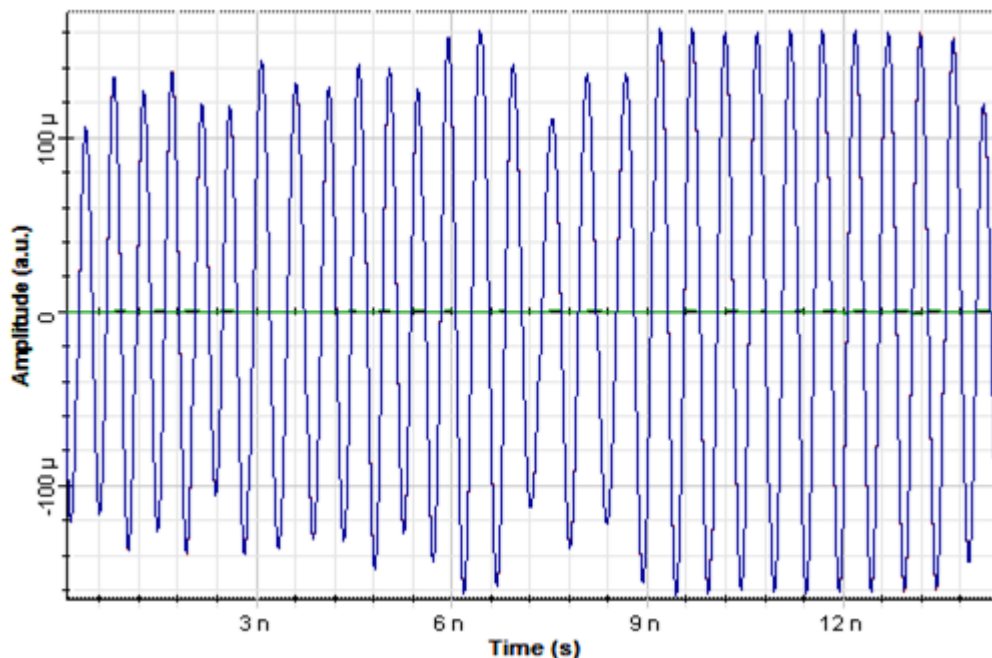


Figure 3- 7: The plot of a band pass filtered received signal in a (0-15ns) interval.

After receiving and filtering the signal, it should be demodulated using a quadrature demodulator. The parameters of the demodulator are configured as shown in Table 3-5.

Frequency indicates the central frequency of the oscillation waves. Cutoff frequency specifies bandwidth of the internal low pass filter.

Parameter	Value
Frequency	2 GHz
Phase	900
Gain	1 dB
Cutoff frequency	0.8 GHz
Filter type	Cosine Roll Off
Roll off factor	0.2

Table 3- 5: The parameters of the quadrature demodulator.

The block diagram of the internal module of a quadrature demodulator components is shown in Figure 3-8.

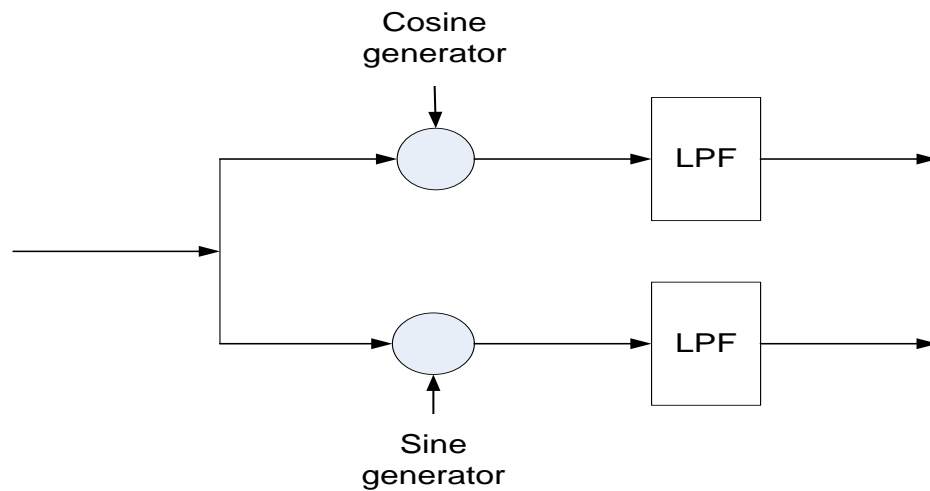


Figure 3- 8: Quadrature demodulator block diagram.

The output of the quadrature demodulator shown in Figure 3-9 is considered to be a base band signal with (I-Q) quadrature components at 1 GHz frequency.

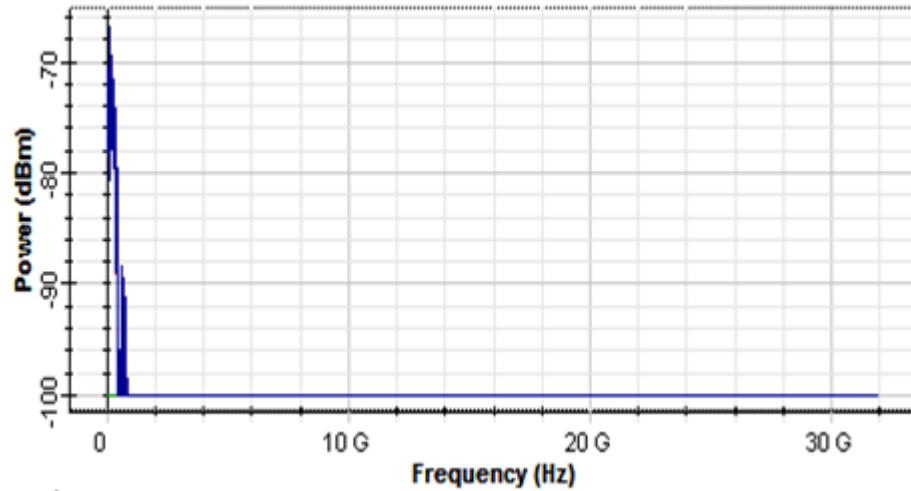


Figure 3- 9: Frequency Spectrum of the demodulated signal.

The plot of a time domain I signal component is illustrated in Figure 3-10, it is clear that signal regeneration is needed to eliminate the signal attenuation and distortion.

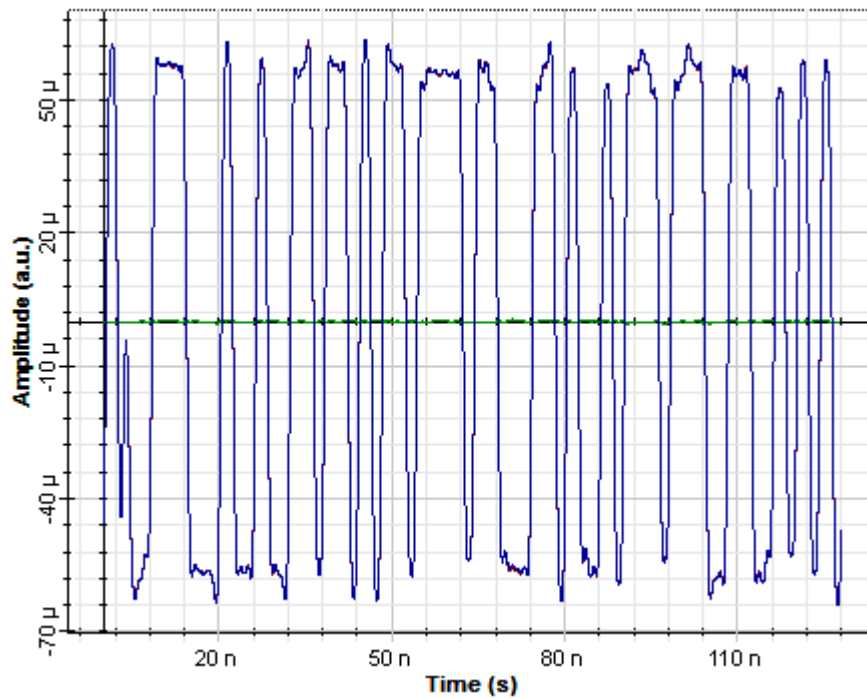


Figure 3- 10: The plot of a time domain demodulated signal.

Now, the signal is duplicated and passed through two output branches, the first branch towards the regenerator and the other towards M-ary threshold detector.

In the first branch: 3R regenerator is used, it has three outputs; the first output port is the bit sequence, the second one is a modulated NRZ signal and the last output is a copy of the input signal. Figure 3-11 illustrates the connection of the internal components of 3R regenerator, it is a subsystem based on the Data Recovery component and a NRZ Pulse Generator. These three signals can be connected directly to the BER Analyzer, avoiding additional connections between transmitter and the receiver stage. 3R regenerator is especially important for WDM systems, where you have multiple transmitters, receivers and BER Analyzers.

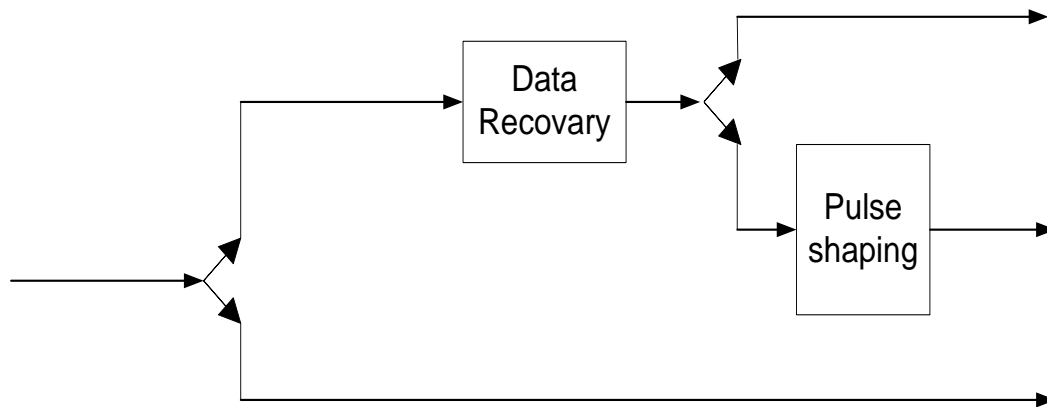


Figure 3- 11: The block diagram of the internal connection of 3R regenerator.

The 3R regenerator is directly connected to BER analyzer to generate the eye diagram of the downlink stage.

In the second branch: M-ary threshold detector is used to decodes multilevel pulses to M-ary signal output, there are thresholds of -0.5, 0.5 and output amplitudes of -1, 0, 1 to compare the electrical signal at a user-defined decision instant with a list of threshold levels. The comparison generates an index used to generate the output amplitude. For example, if the signal input has a value of -0.3, the output level will be 0, since -0.3 is between -0.5 and 0.5. This module is used in the upper part (I- signal) and the lower part (Q-signal), the resultant output is a bit sequence M-ary signal. These two branches feed the PSK sequence decoder, assuming bits per symbol equals 2, then the values for I and Q in case of the initial phase equals to 0 and 45^0 will be as shown in Table 3-6.

Initial Phase = 0			Initial Phase = 45		
I- component	Q- component	Bit sequence	I- component	Q- component	Bit sequence
1	0	00	1	1	00
0	1	01	-1	1	01
-1	0	10	-1	-1	10
0	-1	11	1	-1	11

Table 3- 6: PSK sequence decoder outputs.

After a NRZ pulse shaping to the bit sequence binary signal, the frequency spectrum of signal is shown in Figure 3-12

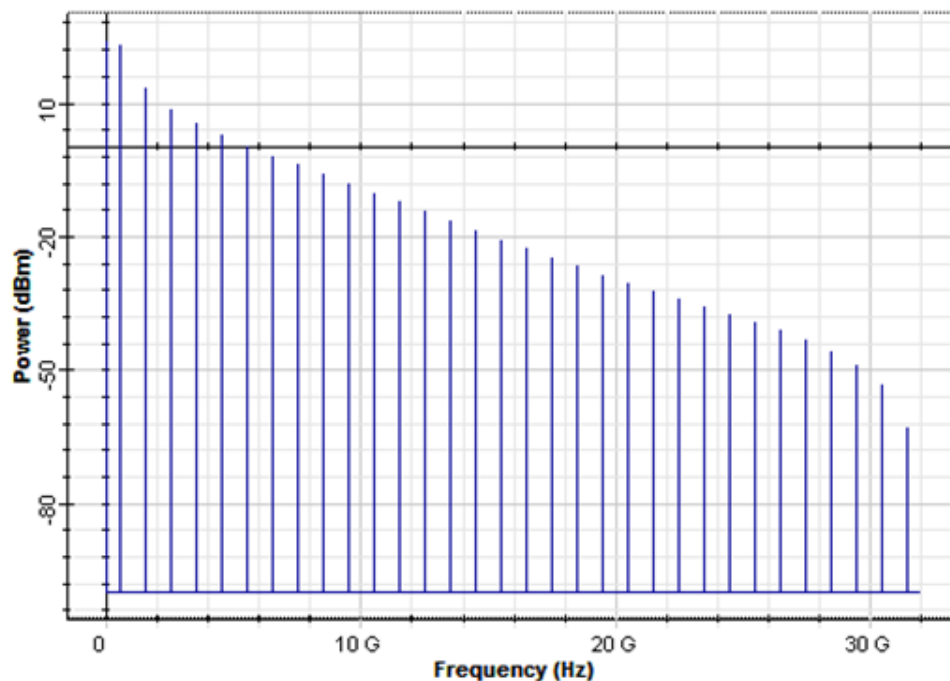


Figure 3- 12: The frequency spectrum of the recovered signal.

3.2.4 RSOA and Uplink Receiver Stage

The Reflective Semiconductor Optical Amplifier (RSOA) performs the functions of not only modulator but also amplifier. It is used for modulations conversion; it performs intensity modulations with no need for local laser source. In general, RSOA has six ports. Here; we use one port to merge the electrical pulse shaped signal at 1 G bps for modulation purpose, another input port is used for optical transmitted OQPSK modulated signal, and

the last output port to outlet the reflected optical intensity modulated signal to reenter the optical fiber cable in the opposite direction. A time delay is used to avoid collisions in a two optical directions. Figure 3-13 illustrates the output reflected signal from RSOA, the noise level in the graph which is due to phase to intensity modulation conversion inside RSOA [7].

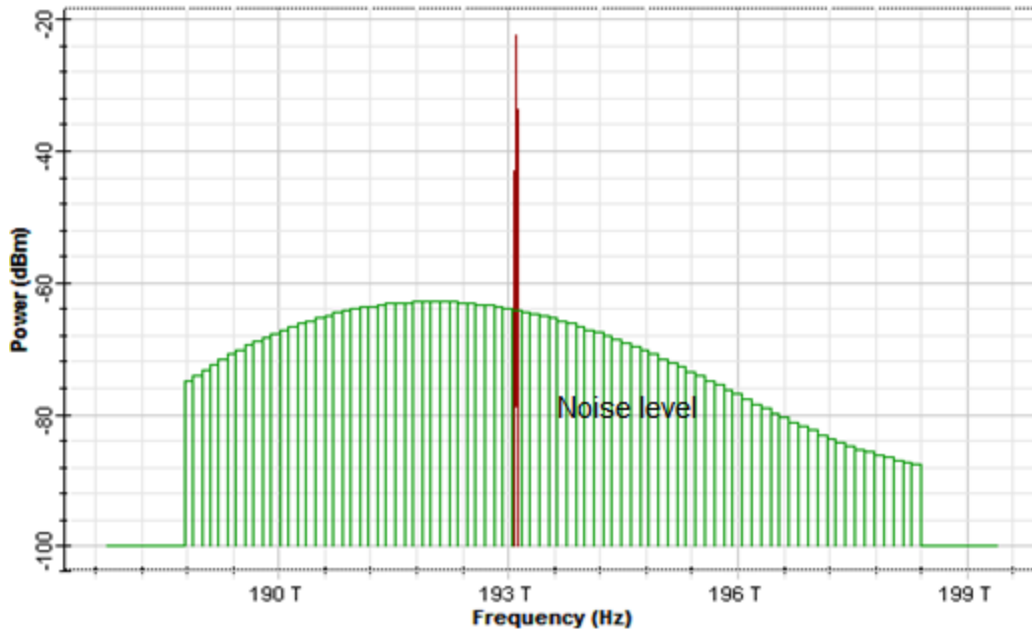


Figure 3- 13:The reflected signal from RSOA.

The uplink receiver consists of a photodetector PD followed by a low pass filter LPF and a 3R regenerator; the BER is displayed at the central office using BER analyzer.

3.2.5 OQPSK Results

In this section, we will discuss the results of OQPSK system in both downlink stage and uplink stage, we will show the influence of the input power variation on the bit error rate BER in both stages , the RSOA gain and noise margin. Also we will discuss the effect of the temperature variation on the BER, RSOA gain and noise figure.

According to the previous section, our system consists of two main stages; the downlink stage or (No- RSOA stage) and the uplink stage or (RSOA stage). Figure 3-14 and Figure 3-15 illustrate the eye diagram of the downstream and upstream signal respectively at input power of 10 dBm.

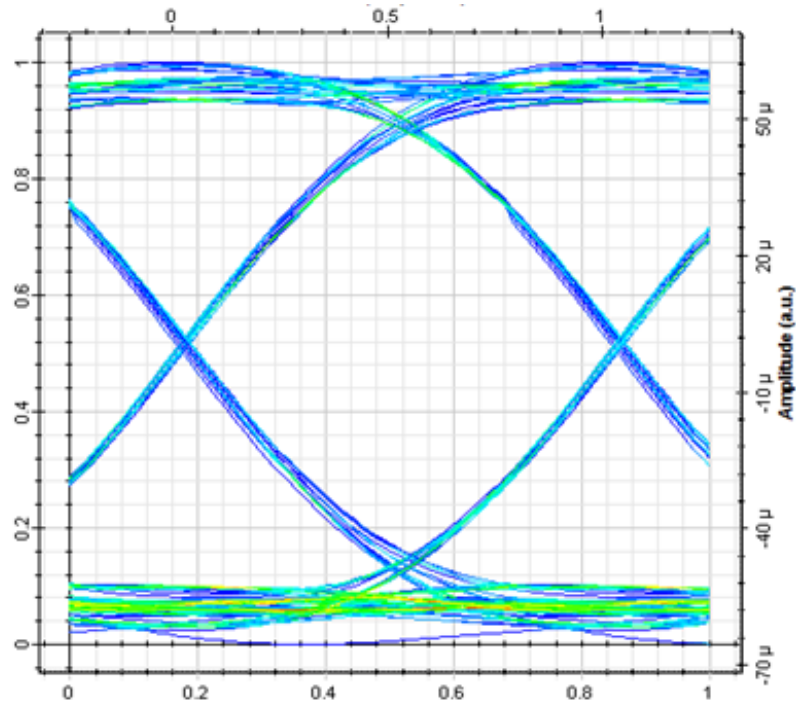


Figure 3- 14: Eye diagram of the downstream signal at input power of 10dBm.

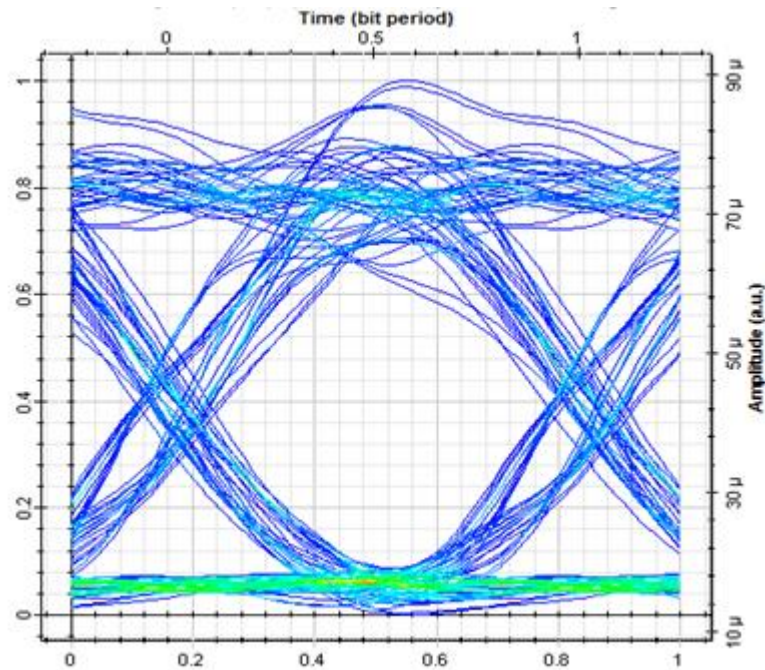


Figure 3- 15: Eye diagram of the upstream signal at input power of 10dBm.

The received eye diagrams of downstream and upstream signals were measured at base station and central office respectively. In both downlink stage and uplink stage, we could see that the eye was clear and open. Though upstream was a thicker when it is compared

with the downstream eye diagram. This could be attributed to the effect of phase to intensity conversion during RSOA injection. Table 3-7 compares between two stages, it is clear that the system performs more efficient in the downstream.

OQPSK Parameter	Uplink	Downlink
Max Q. Factor	6.98425	12.3429
Min BER	1.18664e-012	2.60574e-035
Eye Height	2.92781e-005	4.97788e-005
Threshold	2.65933e-005	1.62944e-006
Decision Instant	0.489474	0.536842

Table 3- 7: Eye Diagram parameters comparison of the Uplink stage and downlink stage

The BER is the number of bit errors divided by the total number of transferred bits during a certain time interval. As the BER decreases the system performance increases and it has a range between 0 to 1.

The BER versus input optical power P_{in} curves for the downlink and uplink are shown in Figure 3-16. It is noted from the figure that the BER for the uplink goes down slowly with increasing P_{in} from -2 dBm to 10 dBm. When $P_{in} = -2$ dBm, the BER = 1.3×10^{-9} and Quality factor (Q) Q=5.9. When $P_{in} = 10$ dBm, the BER = 5.5×10^{-12} and Q= 6.8. For the downlink, the BER goes down quickly with increasing P_{in} from -2 dBm to less than 7 dBm. When $P_{in} = -2$ dBm, the BER = 7.3×10^{-16} and Q= 8. For $P_{in} \geq 7$ dBm, the BER is nearly constant. When $P_{in} = 10$ dBm, the BER = 1.5×10^{-34} and Q = 12.2.

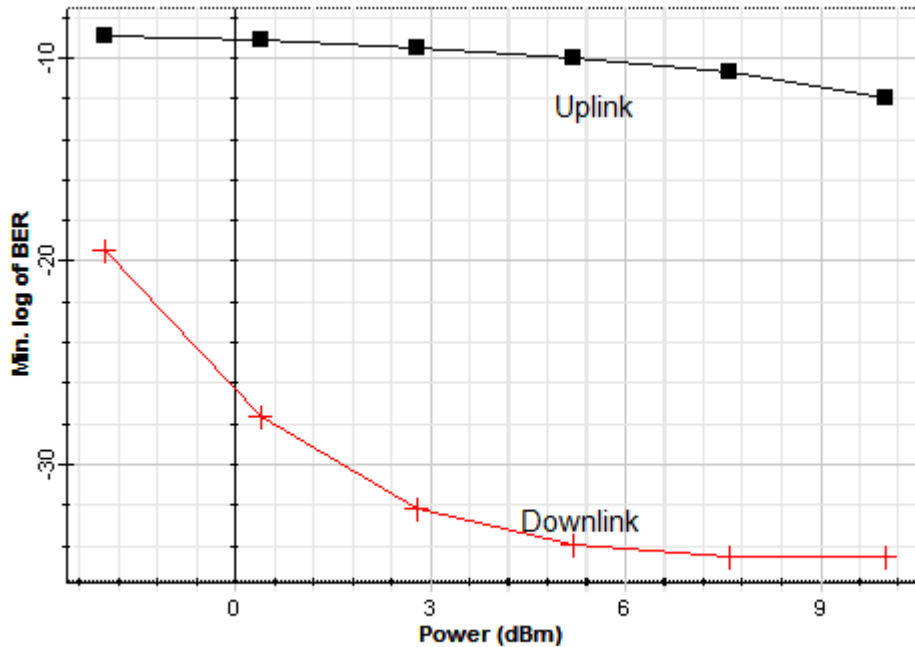


Figure 3- 16:BER versus input power at a fixed temperature (300K)

The Min BER in the down link is 2.6×10^{-34} whereas the Min BER in the uplink is 1.2×10^{-12} . One of the important components in our system is RSOA; it delivers good commercial solutions to reduce the overall system cost since it doesn't need an optical oscillator source to generate the reflected OOK signal and it works as an amplifier at the same time.

Here we study the effect of the variation of input optical power on the RSOA gain; we can measure the RSOA gain in a simple way by measuring the difference between the output optical powers before and after reflection, or using a dual port WDM analyzer. It is clear from Figure 4-17 that as the input power increases from -2 dBm to 10 dBm, the RSOA gain decreases from 29.14 dB to 25.1 dB respectively. Also it is obvious that the gain curve decays smoothly. When $P_{in} = -2$ dBm, the RSOA gain $G_{RSOA} = 29.14$ dB, When $P_{in} = 0.4$ dBm $G_{RSOA} = 28.42$ dB. When $P_{in} = 2.8$ dBm $G_{RSOA} = 27.52$ dB. It is clear that the maximum gain appears at $P_{in} = -2$ dBm, then goes down to reach the lowest gain at $P_{in} = 10$ dBm. This can be explained by the fact that the RSOA is operating in the gain saturation region.

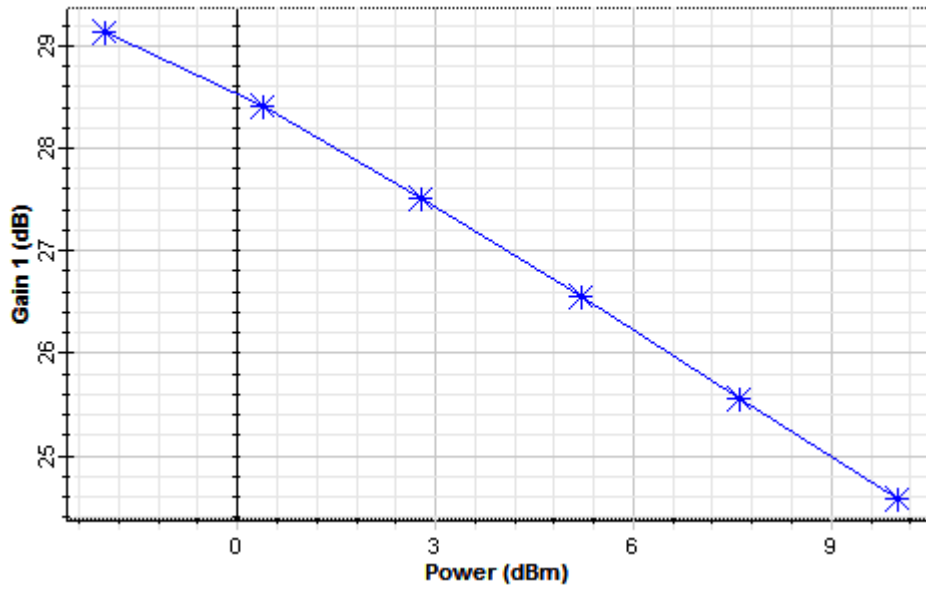


Figure 3- 17: The variation of RSOA gain with input power.

Now, we will study the temperature effect on the BER in up/down streaming, RSOA gain and noise figure. Figure 3-18 illustrates the relationship between the temperature variation and the bit error rate in both uplink stage and down link stage; we can see that the BER is enhanced with increasing temperature in the uplink whereas there is no real effect in the downlink stage since the downstream signal travels through the optical fiber without entering the RSOA. At 273 K the uplink BER = -10.61dB and $Q = 5.7$, while at 330 K BER = 1.3×10^{-14} and $Q = 7.6$.

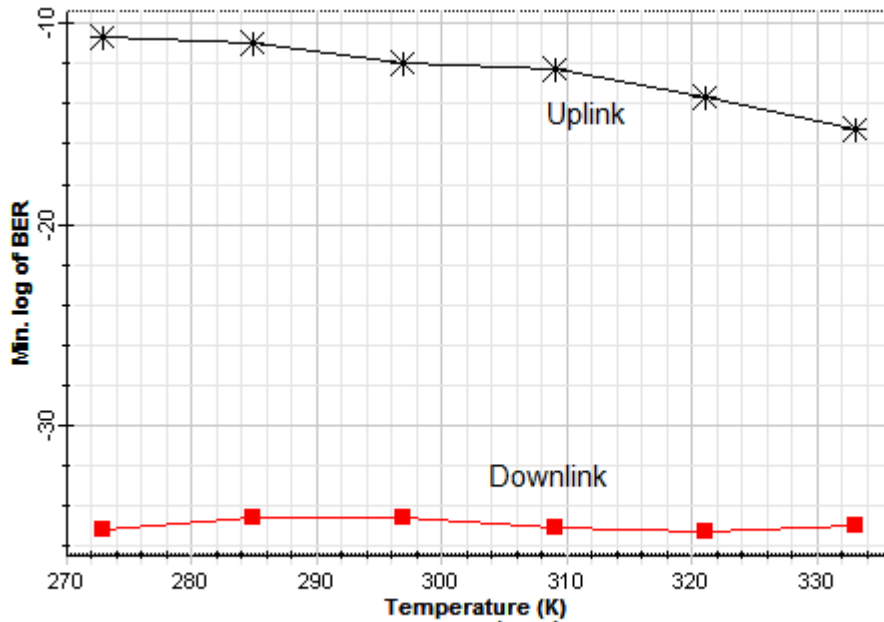


Figure 3- 18: The variation of the BER with temperature.

We also investigated the temperature dependence of the Gain of the RSOA over the temperature range from 273 K to 333 K. The result of temperature dependence of RSOA's gain is shown in the Figure 3-19. It is clear from the figure that the gain decreases linearly as the temperature increases. As the temperature increases the number of free electrons increases which impede the rejected current flow in the RSOA and hence the overall gain decreases.

The noise figure is the difference in decibels (dB) between the noise output of the actual receiver to the noise output of an “ideal” receiver with the same overall gain and bandwidth when the receivers are connected to matched sources at the standard noise temperature T_0 (usually 290 K). The noise power P_n from a simple load is equal to kT_0B , where k is Boltzmann's constant, T is the absolute temperature of the load (for example a resistor), and B is the measurement bandwidth. Noise Factor F is noise-out divided by gain time's noise-in.

$$F = \frac{P_{n \text{ out}}}{kT_0BG1} \quad (4.1)$$

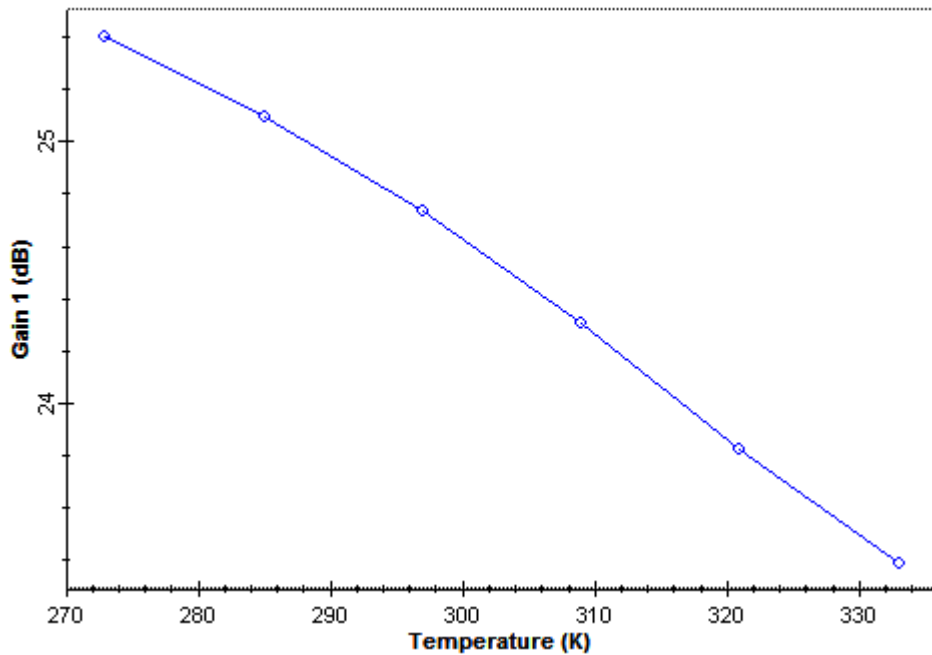


Figure 3- 19: The variation of the BER with temperature.

Noise Factor is a normal realm and noise figure is a logarithmic realm

$$NF = 10 \log_{10} F \quad (3.2)$$

$$NF = P_{out} - (10 \log_{10} B + G_1 - 174) \quad (3.3)$$

Both Table 3-8 and Figure 3-20 illustrate the relation between the temperature and the noise figure, it is obvious that as the temperature increases the noise figure increases in the system; also from the figure and Table 3-8, it is clear that the noise figure increases slowly from T=273 K to T=297 K, then it increases rapidly in the interval T=297 K to T=309 K and it increases exponentially fast from T=310 K to T=333 K. Also it is clear that the simulated results agree with Equation (3.3).

Temperature K	Noise Figure dB
273	0.378092
285	0.386178
297	0.391115
309	0.447799
321	0.602647
333	0.677177

Table 3- 1 : PSK sequence decoder outputs.

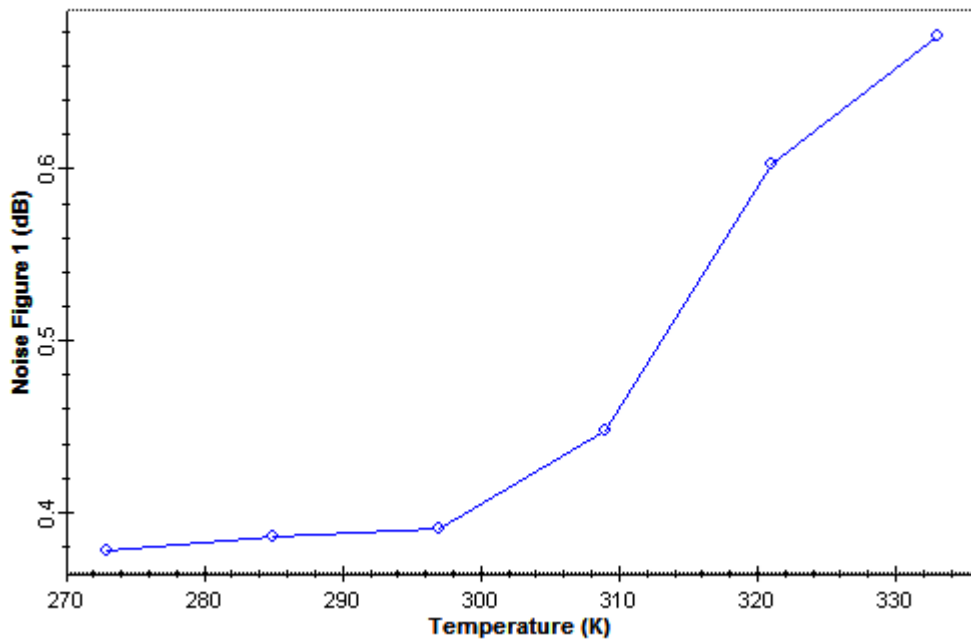


Figure 3- 20: The variation of the noise figure with temperature.

3.3 Differential Phase Shift Keying (DPSK)

In this section, we have demonstrated a bidirectional ROF network based on reflective semiconductor optical amplifier (RSOA) utilizing a Differential Phase Shift keying modulation DPSK signal for down-link and Intensity Modulation (IM) for the upstream stage. We have used the same system modeled in Figure 3-1 but we replace OQPSK modulator by DPSK modulator.

Figure 3-21 demonstrates the Eye diagram for the DPSK downlink stage; it has a clear open eye pattern, an open eye pattern corresponds to minimal signal distortion. Distortion of the signal waveform due to inter symbol interference (ISI) and noise appears as closure of the eye pattern.

The eye diagram for the uplink stage is illustrated in Figure 3-21; we can see that the eye is less open compared with eye pattern illustrated in figure 3-22. However it is a clear (not complete) eye pattern, it includes amplitude (noise) and phase (timing) errors.

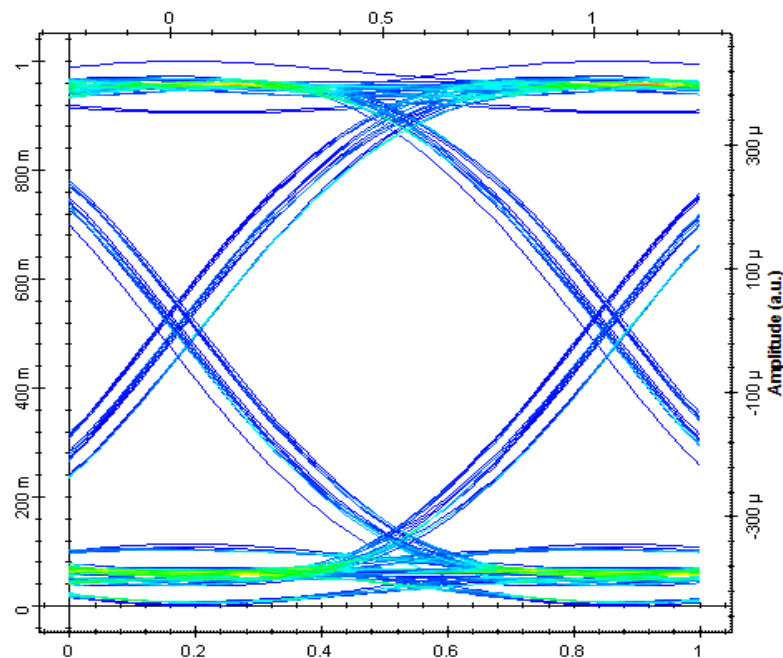


Figure 3- 21:Eye Diagram of DPSK down link stage.

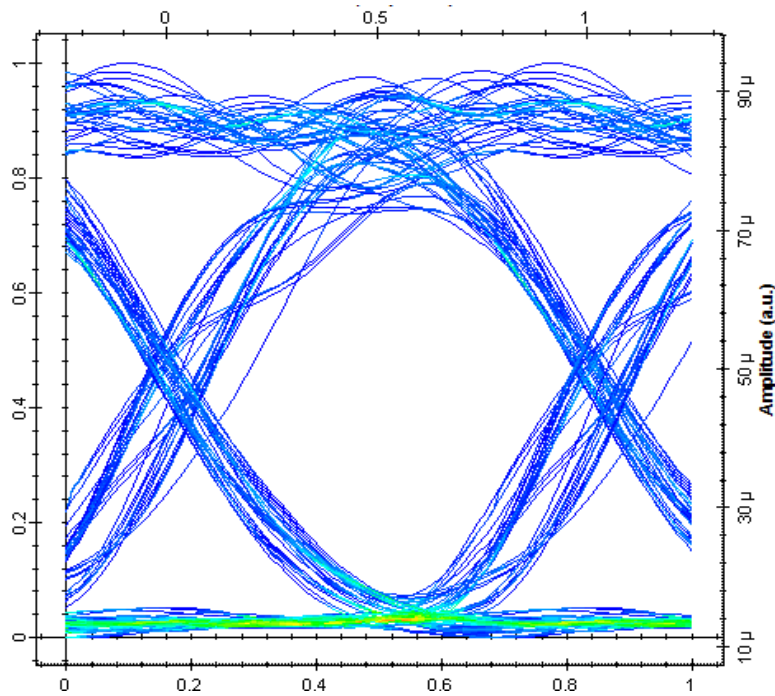


Figure 3- 22:Eye Diagram of DPSK uplink stage.

Now, we will make a detailed comparison between DPSK and an OQPSK. Figure 3-23 displays the measured downstream and upstream BER curves for both DPSK modulation and OQPSK modulation techniques. In general; a minimum acceptable BER rate is about 10^{-12} . Referring to the figure; it is clear that system performance is affected by the power variation; the two systems perform well in region B for the downlink stage and region C for uplink stage. In the uplink, OQPSK performs better than DPSK since its BER curves go down the BER curves of the DPSK.

In the downlink, two systems have nearly the same BER curves form -4dBm to 0 dBm, for input power of more than 0dBm; BER curves of DPSK go down those of OQPSK and the DPSK system performs in a better way.

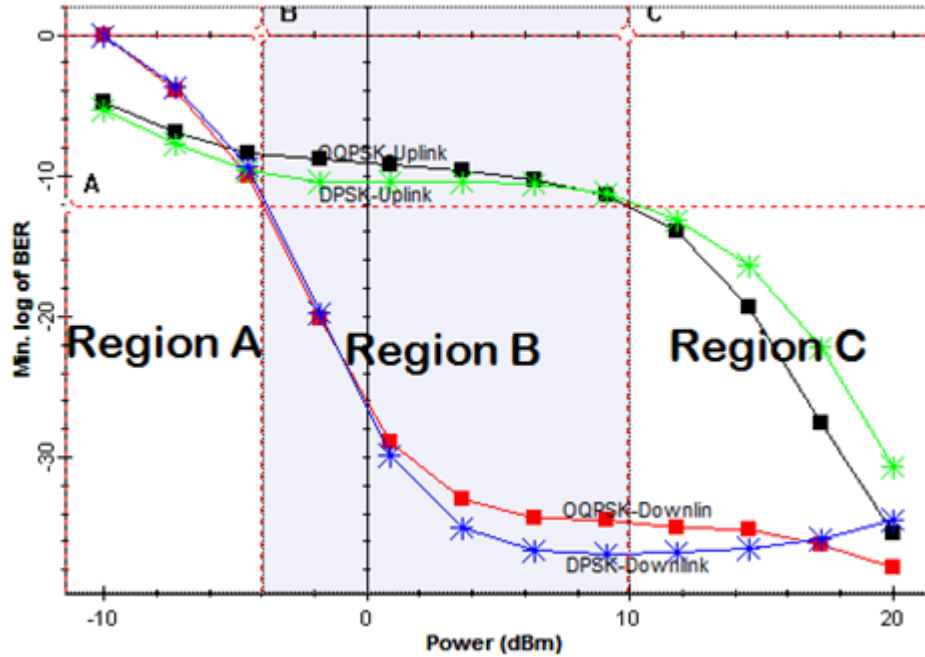


Figure 3- 23: BER curves of OQPSK and DPSK at 300 K.

The RSOA gain is affected by the input power variation, the figure 3-24 below shows the relationship between the input power (dBm) and the RSOA gain (dB) for both OQPSK and DPSK, it is obvious that there is an inverse proportion, that the gain decreases as input power increases. Also it is clear that the DPSK gives larger RSOA gain than OQPSK does for the same input power.

Analysis shows that differential encoding approximately doubles the error rate compared to ordinary M-PSK but this may be overcome by only a small increase in input power. Furthermore, there will also be a physical channel between the transmitter and receiver in the communication system. This channel, in general, will introduce an unknown phase-shift to the PSK signal; in these cases the differential schemes can yield a better error-rate than the ordinary schemes which rely on precise phase information [17].

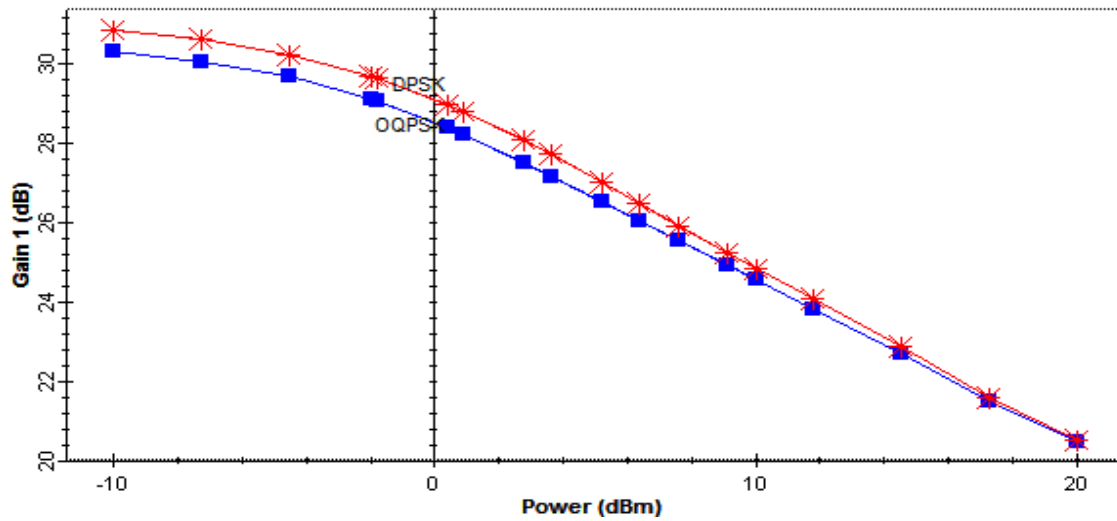


Figure 3- 24:RSOA gain vs. input power for OQPSK and DPSK.

3.4 Subcarrier AM Modulation (SCM-AM)

In this section, consideration is given to the transmission of a high bit rate signal through a single mode fiber system using subcarrier multiplexing (SCM). This high bit rate signal is divided into N_{carrier} small bit rate signals, where N_{carrier} is the number of subcarriers used in the SCM system. The bit-error-rate (BER) of the SCM system for different numbers of subcarriers is determined.

Figure 3-25 shows the proposed WDM-RoF architecture for transmitting subcarrier multiplexing (SCM) encoded channels over a bidirectional single mode optical fiber (50-km). At the central office (CO), a series of narrow bandwidth continuous wave (CW) with various wavelengths are modulated via a LiNbO₃ Mach-Zehnder modulator using 1 Gb/s non-return to zero (NRZ) downstream data to generate downstream signals. Downlink data signal is mixed with local oscillator signal (10-GHz) and a carrier generator having a number of RF subcarriers. The generated SCM signals are multiplexed by Arrayed Waveguide Grating (AWG) and sent over the bidirectional single-mode fiber (SMF). A circulator is used in the Central Office (CO) to separate the downstream and upstream traffic. The SCM signals are de-multiplexed by AWG in Remote Node (RN) where various wavelength lights are sent to different Base stations. Simple AWGs that support both dedicated wavelengths and power-splitting bandwidth sharing are used at the CO and the remote node (RN) [26].

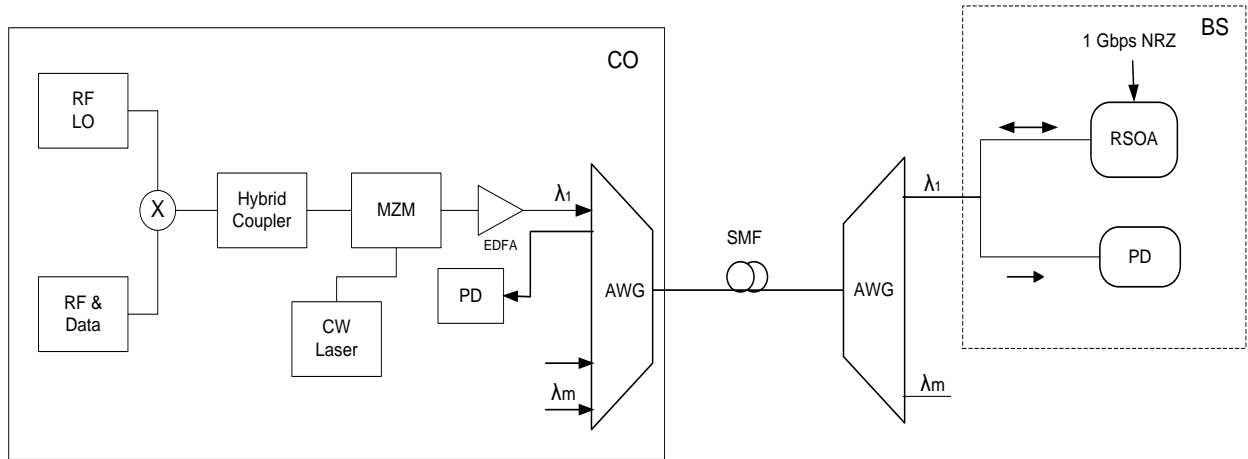


Figure 3- 25:A bidirectional SCM-WDM RoF network.

At the BS, using optical splitter/coupler, portion of the SCM signal is fed to a SCM receiver. For up-link, the other portion of the downstream SCM signal from the splitter/coupler is re-modulated using 1 Gb/s NRZ upstream data by RSOA in the BS. The re-modulated OOK signals are sent back over the fiber to the CO where they are demultiplexed by an AWG DEMUX. The reflected optical signal is detected by a PIN-photodiode. Uplink optical sidebands produce crosstalk when uplink data was detected at central station. Crosstalk can be reduced by using Bessel filter.

The WDM-RoF architecture was modeled using a commercially available package. The proposed scheme uses SCM signal for downstream and OOK signal re-modulated by the RSOA for upstream. The received eye diagrams of downstream and upstream signals were measured at Base station and central office respectively. The received eye diagrams of the downlink and uplink signals are shown in Figure 3-26 and Figure 3-27 respectively. The results show that the Eye closure penalty is smaller for the uplink than that of the downlink which is expected, as the signal travel twice the distance for the uplink. Chromatic dispersion induced by bidirectional fiber will not cause downlink microwave signal a power penalty problem. So, the Maximum eye amplitude for downlink stage after signal transmission took place over 50-km of bidirectional fiber at base station.

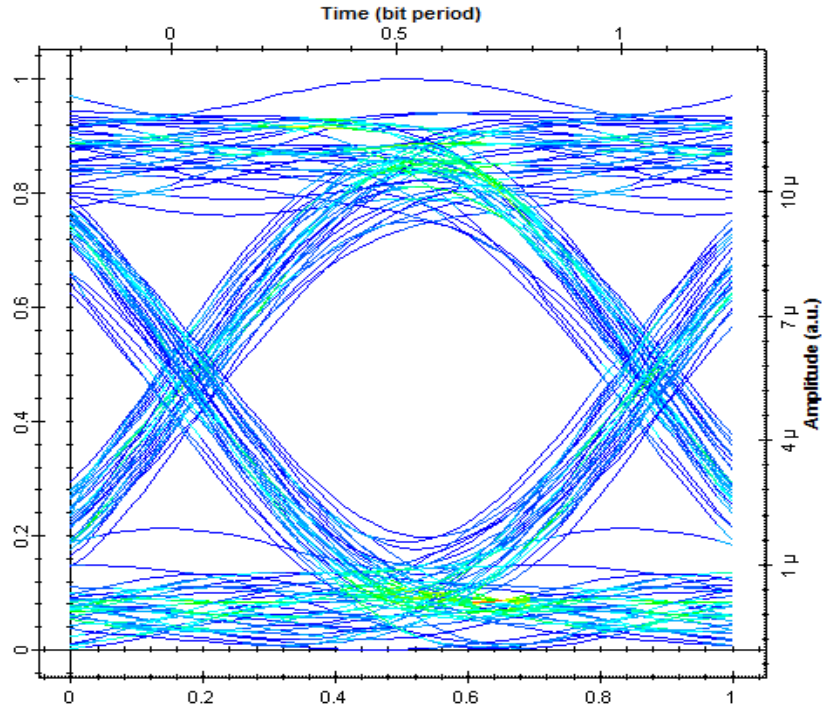


Figure 3- 26:Eye Diagram of the downstream.

BER simulations were carried out for both uplink and downlink with a Bit Rate of 1-Gb/s and no. of subcarriers = 70. The BER variation with input optical power P_{in} curves for the downlink and uplink are shown in Figure 3-28. It is clear that both uplink and downlink do provide good BER performances, however the BER results for the downlink are better than those of the uplink. For example, when $P_{in} = -5$ dBm, the $BER = 1.1 \times 10^{-11}$ for the downlink while it is 2.9×10^{-10} for the uplink. When $P_{in} = +5$ dBm, the $BER = 8.8 \times 10^{-17}$ for the downlink while it is 1.1×10^{-12} for the uplink.

This can be attributed to the mixing noise between unsuppressed SCM signal in downstream and the digital signal of upstream which is generated in the re-modulation process. This noise which influences the upstream signal could be reduced by using low pass filter after the photodetector in the CO.

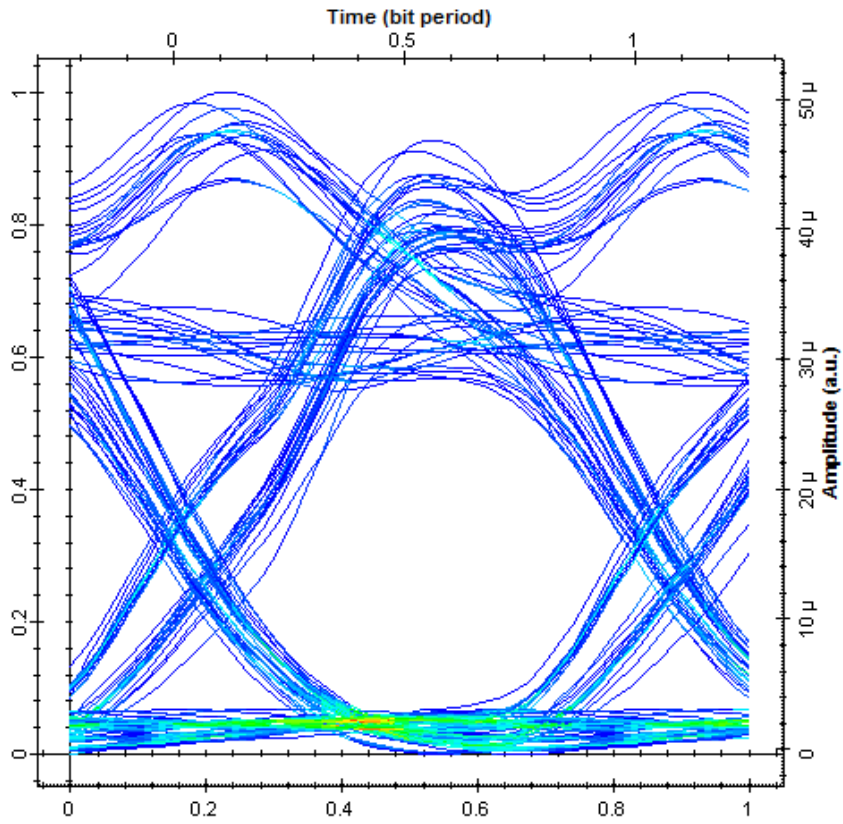


Figure 3- 27:Eye Diagram of the upstream.

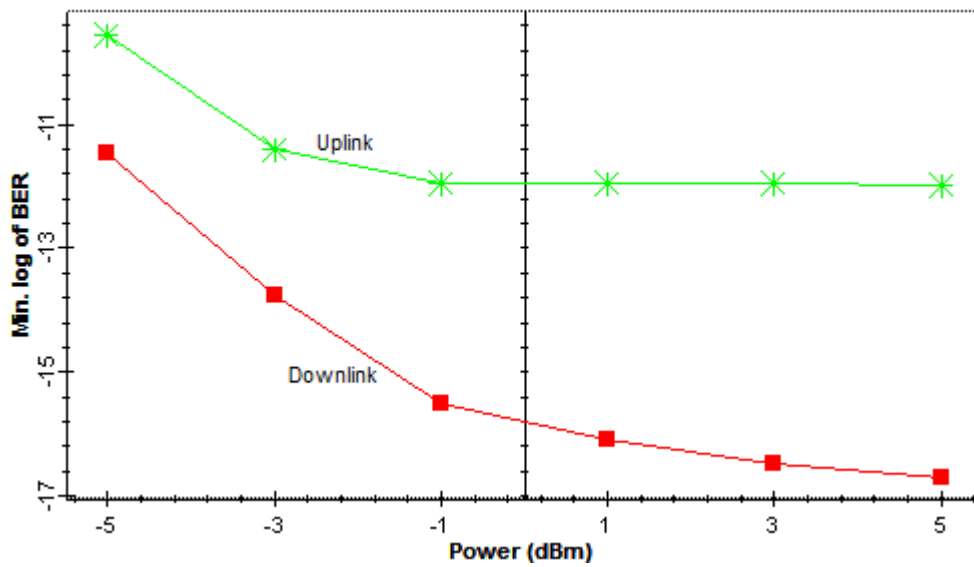


Figure 3- 28:BER vs. input power for uplink and downlink.

It is also noted from the figure that the BER for the uplink stays nearly constant for $P_{in} \geq -1$ dBm. This can be explained by the fact that the RSOA is operating in the gain saturation region.

The variation of the gain of RSOA with the optical input power P_{in} is shown in Figure 3-29. It is clear that the maximum gain appears at $P_{in} = -5$ dBm, then goes down to reach the lowest gain at $P_{in} = -1$ dBm where it goes into saturation.

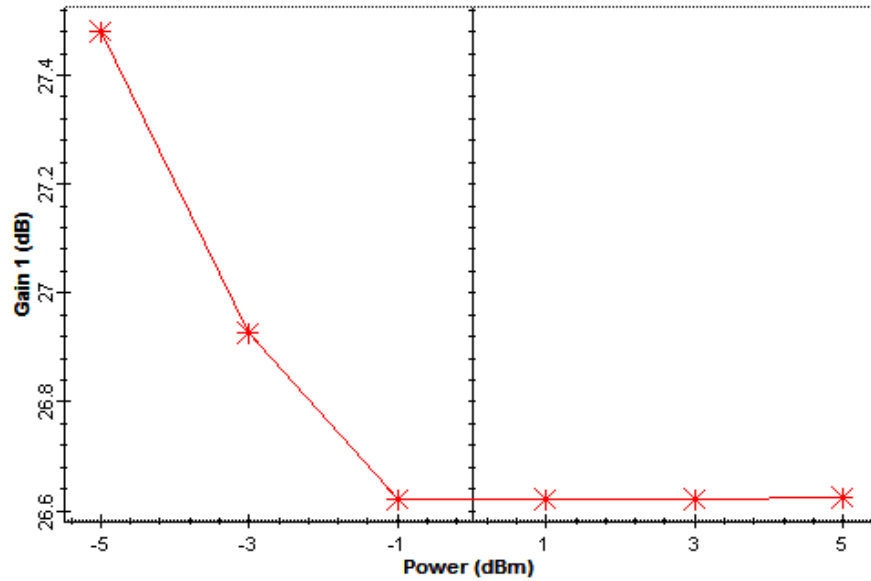


Figure 3- 29:Gain vs. input power at a fixed temperature.

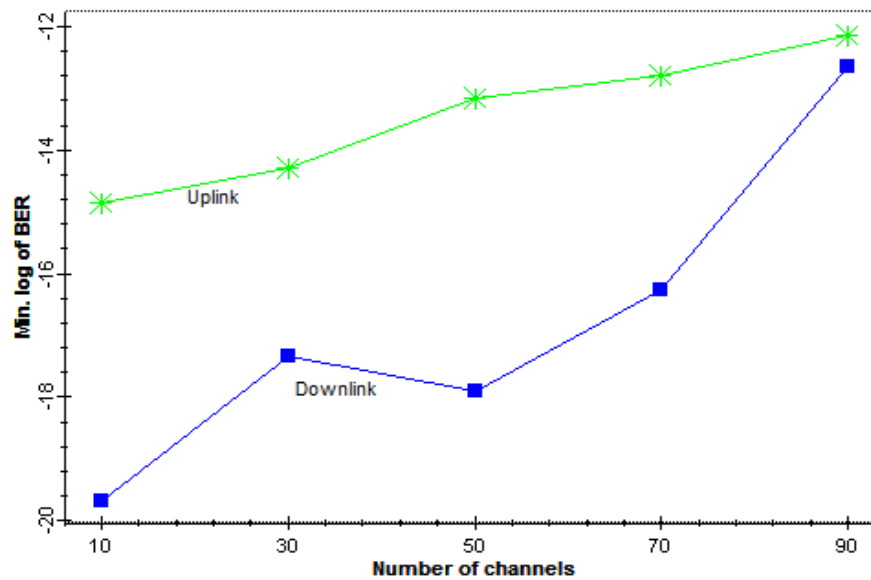


Figure 3- 30:BER of SCM vs. Number of channels at a fixed input power.

The variation of BER with no. of subcarriers is plotted in Figure 3-30. It is clear from the results that increasing the number of subcarrier channels degrade the system performance. For example, when RF channels increase from 10 to 90, corresponding BER decreases from 4.6×10^{-21} to 5.3×10^{-14} for the downlink, while it decreases from 1.4×10^{-15} to 7.3×10^{-13} for the uplink. This can be explained by the fact that, as the number of sub-carrier channels increases, their frequency spacing decreases which results crosstalk or noise [25]. There is unexpected behavior of the system when the number of channels 30 channel, it may be due to simulation error.

3.5 Orthogonal Frequency Division Multiplexing (OFDM)

Radio-over-fiber (RoF) technology has several benefits such as larger bandwidth, reduced power consumption etc. that has made it an attractive implementation option for various communication systems. Orthogonal Frequency Division Multiplexing (OFDM) is seen as the modulation technique for future broadband wireless communications because it provides increased robustness against frequency selective fading and narrowband interference, and is efficient in dealing with multi-path delay spread. This section investigates the feasibility of OFDM as a modulation technique to transmit the baseband signal over fiber. Laser diode and photodiode have been modeled and used as optical transmitter and optical receiver respectively. The model can be used with different wireless communication systems such as Wireless LANs and Digital Video Broadcasting (DVB) and it is supporting to the 4th generation cellular systems [27].

In this work we develop and simulate OFDM RoF system, RoF realize the transparent transform between RF signal and optical signal. The input random binary digits are modulated by 4-QAM combined with OFDM technology which is shown in Figure 3-31. An OFDM signal at 7.5 GHz carrier frequency is then modulated by MZM (Mach Zehnder Modulator) to the 1550 nm optical carrier generated by CW laser.

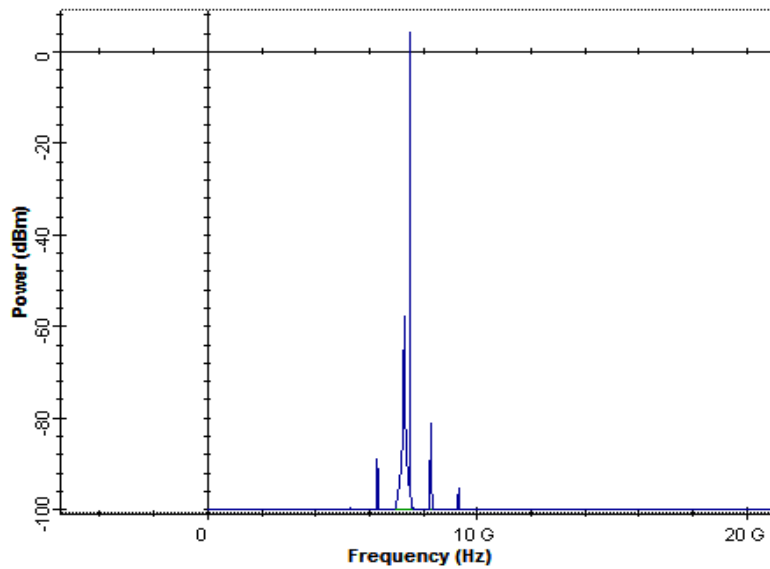


Figure 3- 31:Frequency domain presentation of OFDM signal.

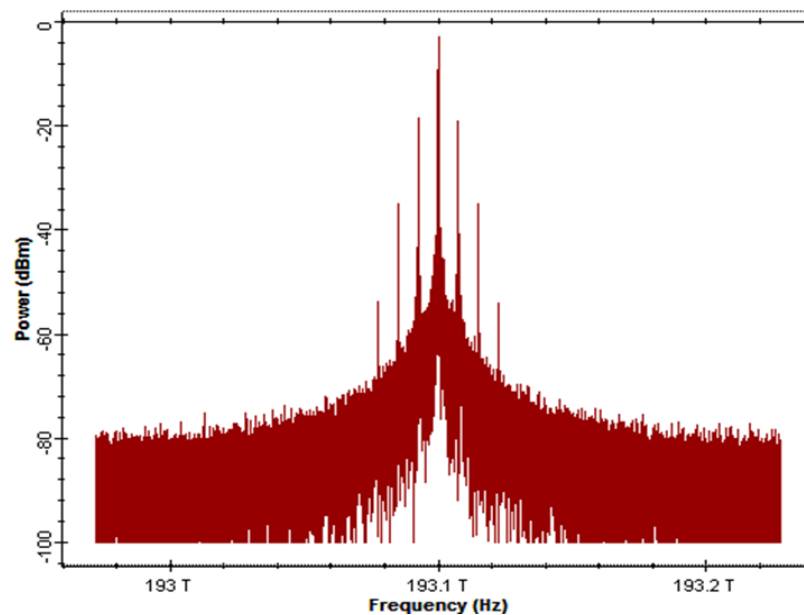


Figure 3- 32:Frequency domain presentation of transmitted signal.

The optical transmitted singles are shown in Figure 3-32, they travel through the optical fiber of 50km length, and are turned back into the microwave through O/E transformation in a PIN photodiode, and then binary digits can be obtained through OFDM-demodulation, the received downlink eye diagram is shown in Figure 3-33.

In uplink, a portion of the downstream OFDM signal is re-modulated using 1 Gb/s NRZ upstream data by RSOA in the BS. The re-modulated OOK signals are sent back over the fiber to the CO. The reflected optical signal is detected by a PIN-photodiode. Figure 3-34 shows the eye diagram of the uplink stage, it is a clear opened eye.

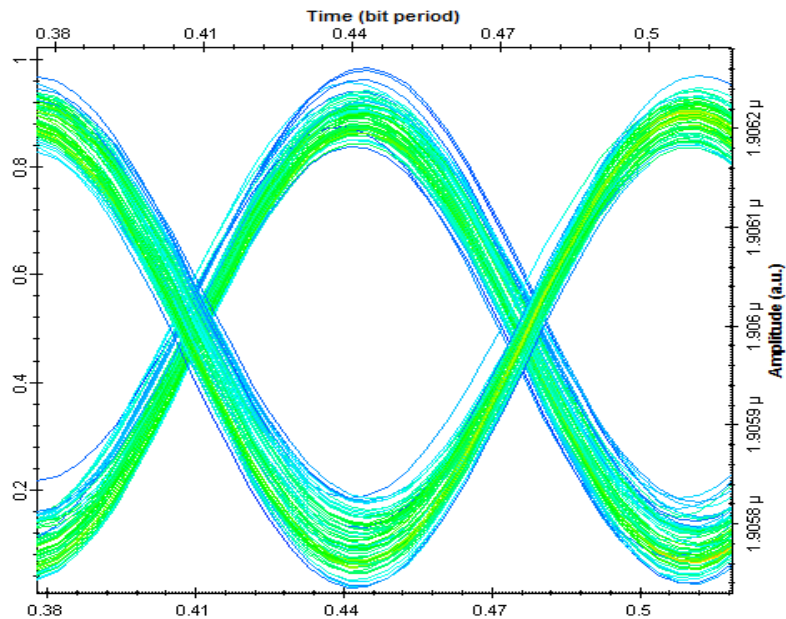


Figure 3- 33:Eye diagram of the downlink stage.

In this part, we will focus on the transmission performance analysis in the optical fibers. The wave forms of the optical pulses are influenced by attenuation, dispersion and nonlinear effect. Figure 4-36 shows the graph of log of BER versus input optical power of CW laser for fiber length $L = 50$ km. This simulation is performed to find the suitable input power of the CW laser. Acceptable BER is below 10^{-10} ($BER < 10^{-10}$). As a first step we set the range of input power from -10 dBm to 10 dBm to show the system behavior, and then we plot the BER curves with input power from -5 dBm to 1 dBm, it is clear from Figure 3-35 that the BER curves of the uplink stage are a better than those of downlink stage, it is 40 dB apart. Also it is clear that BER decreases as input power increases, it is known that the error occurs as the power of the received signal exceeds the threshold power level, for instant; the power level is 0 dB and the transmitted power is 3 dB, so if the received power is -1 dB (due to absorption, reflection or noise power), then the receiver detects an error [28]. So that the increased input power reduce the BER.

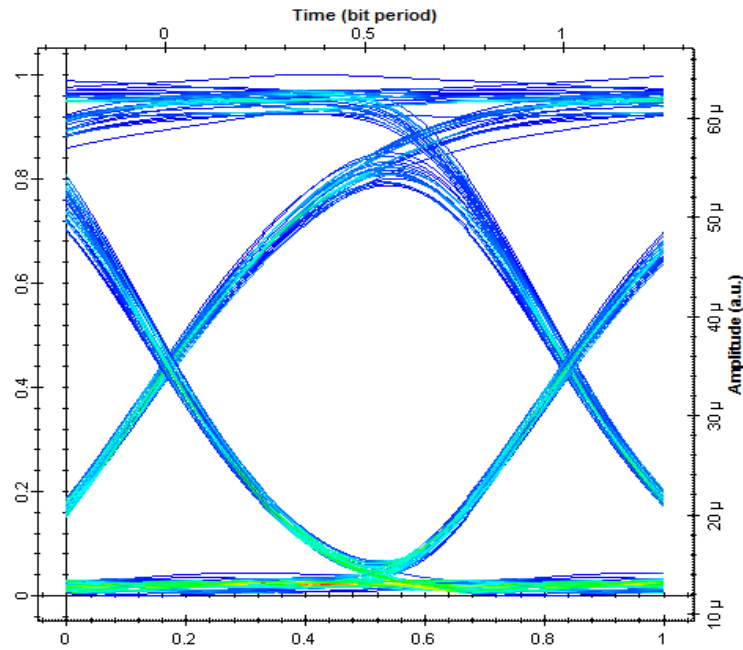


Figure 3- 34:Eye diagram of the uplink stage.

Here we plot the variation of the BER with the number of channel, Figure 3-37 indicates that the BER in the downlink stage is nearly constant from 10 subcarriers to 90 subcarriers, decreases slowly from 90 subcarriers to 210 subcarriers and increases rapidly from 210 subcarriers to 290 subcarriers.

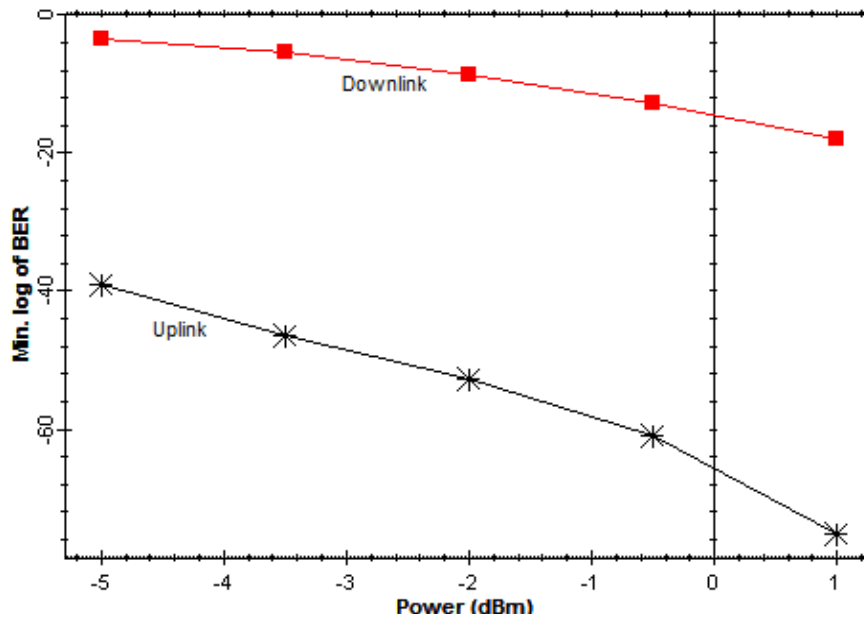


Figure 3- 35:The variation of the BER with input power.

In the uplink; the BER increases rapidly for lower than 100 subcarriers, then the system performs regularly stable for more than 100 subcarriers. In general; we can say that; as the

number of subcarriers increases, then the level of crosstalk increases and degraded overall performance of simulative model and BER increases, this is due to their frequency spacing decreases which results crosstalk or noise.

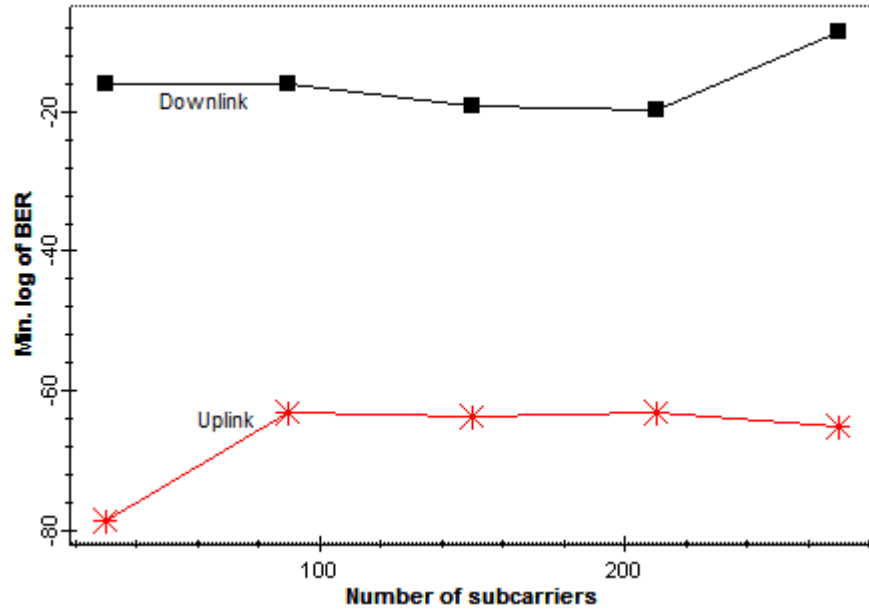


Figure 3- 36: The variation of the BER with number of subcarrier.

Chapter 4 –Conclusion

4.1 Summary

In this thesis, we have designed and implemented a bidirectional radio over fiber ROF system based on RSOA for uplink stage, different types of modulations have been used. Our system is a very effective solution for wireless systems due to increasing the demand for multiservice operation and hence broadband access, it is a reliable and cost effective communication system that can support anytime, anywhere, and any media are needed. It is able to alleviate the increasing demand for high-bandwidth services.

The first part in our work introduces a novel bidirectional RoF network utilizing a 1 Gb/s OQPSK signal for down-link and a 1 Gb/s OOK signal for up-link. RSOA has been used for re-modulation of a down-link signal over 50 km SMF. Moreover, the RSOA is cost-effective since it performs the functions a modulator (no need for local laser source) and an amplifier. We also investigated the impact of the temperature dependency of the RSOA on upstream data. Moreover; we use another modulation technique (DPSK) and compare the results of the two systems. The results obtained showed that the temperature had a significant impact on performance of ROF system. Also, it showed that the proposed system has potential application in next-generation convergent wireless-wired optical network.

The second part has been proposed as a solution for increasing bandwidth demand. The combination of WDM and SCM has been performed to provide high data rates and bandwidth in wireless communication. We have analyzed the performance of WDM/SCM Radio over Fiber System. We presented a demonstration of 1Gb/s signal for up/downstream in 50-km bidirectional link. The upstream traffic is obtained by re-modulating the downstream traffic at the BS. The results obtained here show that increasing total number of sub-carriers channels has a significant impact on performance of WDM-SCM ROF system. The most significant advantage of SCM in optical communications is its ability to place different optical carriers together closely. On the other hand, Wavelength Division Multiplexing (WDM) is a multiplexer at the transmitter to join the signals together, and a de-multiplexer at the receiver to split them apart. In

WDM each laser is modulated at a given speed, and the total aggregate capacity being transmitted along the high-bandwidth fiber is the sum total of the bit rates of the individual lasers.

Finally we discuss the proposed OFDM-RoF model. The whole hierarchical simulation system model was constructed and simulated successfully using a commercial optical system simulator. By varying both the input optical power and the number of subcarriers, the log of bit-error-rate (BER) can be achieved. The results obtained here show that the combination of OFDM technology and ROF technology makes it possible to transform the high speed RF signal to the optical signal, so that the optical fibers with broad bandwidth can be used. The OFDM technology, at the same time, was showing its advantages in speeding up the signal processing; it is also being focused in 4G wireless communication system.

4.2 Suggestion for Improvement

The design in this thesis can be upgraded to give better performance. To increase the system efficiency, the data rate and the operating frequency can be increased. We use a 1G b/s data rate, this will definitely increases to 10 Gb/s. Also the design can be modified to operate with other modulation techniques.

Finally, the designed system should be extended to carry code multiplexed systems such as Code Division Multiplexing Access (CDMA) systems, which plays a role in future broadband wireless system.

References

- [1] J. Part, C. Arellano and C. Bock, "Optical network unit based on a bidirectional reflective semiconductor optical amplifier for fiber-to-the-home networks," *IEEE Photon*, vol. 17, no. 1, pp. 250-252, Jan. 2005.
- [2] G. C. Kassar, N. Calabretta, and I. T. Monroy, "Simultaneous optical carrier and radio frequency re-modulation in radio-over-fiber systems employing reflective SOA modulators," in *Lasers and Electro-Optics Society*, Lyngby, Oct. 2007, pp. 798-799.
- [3] Gerd Keiser, *Optical Fiber Communication*, 3rd ed., International Editions, Ed.: McGraw Hill, 2000.
- [4] B. Carbon, V. Girod and G. Maury, "Optical Generation Of Microwave Functions," in *Microwave Photonics for Emission and Detection of Broadband Communication Signals*, Belgium, 2001.
- [5] M. Webster, G. Wimpenny, K. Beacham and L. Crawford D. Wake, "Radio over fiber for mobile communications," *IEEE*, vol. 4, no. 2, April 2004.
- [6] Fady El-Nahal, "Bidirectional WDM-Radio over Fiber System with Sub Carrier Multiplexing Using a Reflective SOA and Cyclic AWGs," (*IJACSA*) *International Journal of Advanced Computer Science and Applications*, vol. 2, no. 8, pp. 93-96, August 2011.
- [7] Xianbin Yu, Timothy Braidwood Gibbon, and Idelfonso Tafur Monroy, "Bidirectional Radio-Over-Fiber System With Phase-Modulation Downlink and RF Oscillator-Free Uplink Using a Reflective SOA," *IEEE*, vol. 20, no. 24, pp. 2180-2182, Dec. 2008.
- [8] M.C.R. Medeiros, R. Avo, P. Laurencio, N.S. Correia, A. Barrada, H.J.A. da Silva I. Darwazeh, J.E Mitchell and P.M.N Monteiro, "Radio over Fiber Access Network Architecture Employing Reflective Semiconductor Optical Amplifiers," *IEEE*, 2007.
- [9] Arief M., Sevia M. Idrus and S. Alifah, "The SCM/WDM System Model for Radio over Fiber Communication Link," in *INTERNATIONAL RF AND MICROWAVE CONFERENCE PROCEEDINGS*, Kuala Lumpur, MALAYSIA, Dec. 2008, pp. 344-347.
- [10] N. Mohamed', S.M. Idrus², A.B. Mohammad^{3*} and H. Harun, "Millimeter-Wave Carrier

Generation System for Radio over Fiber," in *Microwave conference proceedings*, Kuala Lumpur, August 2008, pp. 111-115.

- [11] Cristina Arellano, Carlos Bock, and Josep Prat, "RSOA-based Optical Network Units for WDM-PON," in *Optical Society*, America, 2005, pp. 1-3.
- [12] J. Capmany, D. Pastor, A. Leon, P Chamorow, and D. Santos, "Experimental demonstration of optical prefiltering in WDM-SCM optical networks employing ultraselective optical bandpass filter," *Electronic Letters*, vol. 35, no. 4, pp. 318-319, 1999 February.
- [13] Jianping Wang, Xianwei Zhou, Yongxia Xu, Wen Wang, "Performance Improvement of OFDM-ROF System with Clipping and Filtering Technique," *IEEE*, vol. 54, no. 2, pp. 196-199, May 2008.
- [14] M. Kang and S.K. Han, "A novel hybrid WDM/SCM-PON sharing wavelength for up and down link using reflective semiconductor optical amplifier," *IEEE Photon*, vol. 18, no. 3, pp. 502-504, Feb. 2006.
- [15] C. Lim, A. Nirmalathas, D. Novak and R. Waterhouse, "Millimeter-wave broad-band fiber-wireless system incorporating baseband data transmission over fiber remote LO delivery," *Light wave Technology*, vol. 18, no. 10, pp. 1355-1363, 2004.
- [16] C. H. Cox, E. I. Ackerman, G. E. Betts, and J. L. Prince, "Limits on the performance of RF-over-fiber links and their impact on device design," *IEEE*, vol. 54, no. 2, pp. 906-920, Feb. 2006.
- [17] A.J. Lowery, L. Du, J. Armstrong, "Orthogonal frequency division multiplexing for adaptive dispersion compensation in long haul WDM systems," in *Optical Fiber Communications Conference*, Anaheim, 2006, p. 39.
- [18] B. Djordjevic and B. Vasic, "Orthogonal frequency division multiplexing for high-speed optical transmission," *Optics Express*, vol. 14, no. 9, pp. 3767-3775, April 2006.
- [19] Nee R. van., and Prasad R., *OFDM For Wireless Multimedia Communications*, 1st ed. Boston, London: Artech House , 2000.

- [20] B. J. Dixon, R.D. Pollard, and S. Iezekiel, "Orthogonal frequency-division multiplexing in wireless communication systems with multimode fiber feeds," *IEEE*, vol. 49, no. 8, pp. 1404-1409, 2001.
- [21] Simon Haykin, *Digital Communications.*, Third Edition ed. Toronto, Canada: John Wiley & Sons, 1988.
- [22] John G. Proakis, *Digital Communications*, Third Edition ed. Singapore: McGraw Hill, 1995.
- [23] Couch, Leon W. , *Digital and Analog Communications*, 6th ed. Upper Saddle River, USA: Prentice-Hall, 1997.
- [24] Minhong Zhou, "Novel Modulation Technique for Radio-over-Fiber Systems," Concordia University, Canada, Thesis 978-0-494-40900-8, 2007.
- [25] Fulvio Grassi, José Mora, Beatriz Ortega, José Capmany, "Experimental Evaluation of the Transmission in a Low Cost SCM/WDM Radio over Fibre System Employing Optical Broadband Sources and Interferometric Structures," in *ICTON*, Island, 2008, pp. 1-4.
- [26] Hyun-Seung Kim, "Bidirectional WDM-RoF Transmission for Wired and Wireless Signals," in *Proc. of SPIE-OSA-IEEE* , Asia, 2009, pp. 76320-76322.
- [27] Y.-M. Lin and P.-L. Tien, "Next-Generation OFDMA-Based Passive Optical Network Architecture Supporting Radio-Over-Fiber," *IEEE*, vol. 28, no. 6, pp. 791-799, 2010.
- [28] A.H.M. Razibul Islam, Md, Imrul Hassan and Ju Bin Song, "Adjacent channel power ratio of OFDM signals for broadband convergence networks," in *Joint International Conference on Optical Internet and*, Korea, 2006, pp. 180-182.
- [29] M.D. Feuer, J.M. Wiesenfeld, J.S. Perino, C.A Burrus, G. Raybon, S.C. Shunk, and N.K. Dutta, "Single-port laser-amplifier modulators for local access," *IEEE Photon*, vol. 8, no. 9, pp. 1175-1177, Sep. 1996.
- [30] N. Buldawoo, S.Mottet, F.Le Gall, D. Sigonge, D. Meichnin, and S. Chelles, "A semiconductor laser amplifier-reflector for the future FTTH applications," in *Proc. Eur. Conf. Optical Communication*, Edinburgh, U.K., 1997, pp. 196-199.

- [31] T. Kuri, K. Kitayama, and Y. Takahashi, "A single light-source configuration for full-duplex 60-GHz-band radio-on-fiber system," *IEEE*, vol. 51, no. 2, pp. 431-439, Feb. 2003.
- [32] M. R. Salehi, Y. Le Guennec, and B. Cabon, "Signal and noise conversions in RF-modulated optical links," *IEEE*, vol. 52, no. 4, pp. 1302-1309, April 2004.
- [33] M. Sauer, A. Kobayakov, and J. George, "Radio over fiber for picocellular network architectures," *Light Wave Technology*, vol. 25, no. 11, pp. 3301-3320, Nov. 2007.
- [34] F. Bucholtz, P. S. Devgan, J. D. Micknney, and K.J. Willams V.J. Urick, "Phase modulation with interferometric detection as an alternative to intensity modulation with direct detection for analog-pho-tonic links," *IEEE*, vol. 55, no. 9, pp. 1978-1985, Sep 2007.